nature portfolio

Peer Review File

Structural basis of K11/K48-branched ubiquitin chain recognition by the human 26S proteasome

Corresponding Author: Dr Shang-Te Danny Hsu

This file contains all reviewer reports in order by version, followed by all author rebuttals in order by version.

Version 0:

Reviewer comments:

Reviewer #1

(Remarks to the Author)
In this manuscript, Draczkowski and colleagues present a cryo-EM study of human 26S proteasome associated with a model ubiquitinated substrate. The authors engineer the process of in vitro ubiquitination in order to generate the substrate modified with K11/K48-branched ubiquitin chains, a type of heterotypic chain with reported enhanced degradation and affinity towards the proteasome, and a partially characterized mode of interaction with proteasomal ubiquitin receptors. With this approach, the authors obtain multiple conformational variants of the 26S – substrate complex with a very good definition of up to four ubiquitin molecules defining the K11/K48-branch, and uncover and nicely describe a putative novel K11/K48-branched ubiquitin interaction region, based on a conserved motif in Rpn2 subunit and on multiple adjacent surfaces of neighbor subunits.

One notorious experimental paradox in the field is that, in a context of deficiency in the described (and well-characterized) proteasomal ubiquitin receptors (RPN10 [UIM], RPN13 [PRU] and RPN1 [T1]), and in the absence of substrate UBL-UBA shuttles, 26S proteasomes are still capable to degrade ubiquitinated substrates. Based on that, it has been hypothesized that at least one additional ubiquitin-binding surface must be hidden in the regulatory particle of the 26S. In this work, the authors claim having discovered this cryptic ubiquitin recognition site, which appears to be sculpted to bind K11/K48-branched Ub species.

Furthermore, the work is rich in detailed data which describe important additional aspects that help to comprehend the interaction of distinct ubiquitin moieties of polyubiquitinated proteins with the subunits of the RP of the proteasome.

Overall, the work is very well designed and the data presented is outstanding, with profound analysis and discussion. Referenced bibliography is fine (however some suggestions are added).

Said that, since the work is focused on a unique approach, without additional functional validations of the discoveries (for example, mutations of key positions), the current version is placed in the borderline of acceptance in Nat Comms, from the stand point of this reviewer. The feeling is that the high quality of the data could make this work acceptable after addressing the following issues (which could be defined as “minor”)

Main issues that should be addressed are:

1. The experimental approach includes a well-designed plan to integrate Rpn13 and inactive UCHL5(C88A) in the whole reconstituted 26S-Sic1PY-Ubn(K63R)-UCHL5(C88A) complex. However, the reconstitution evidence shown (Supplementary Fig. 2) are not clear and panels have some problems. Panel A shows native gels cut. It is important to know whether the lanes correspond to the same electrophoresis run, otherwise it’s impossible to know that the shift is real. In panel B, it is not shown a Rpn13 western blot. Did proteasomes before reconstitution contain endogenous Rpn13 and UCHL5? It is also puzzling that the RP-CP show no WB signal for Ub and UCHL5, Do authors have an explanation for that? Additionally, UCHL5 could not be resolved in the EM structures obtained (this point is discussed by authors), but nothing is mentioned about Rpn13. Could Rpn13 be resolved? When authors mention that (line 149): “Nonetheless, such functional dynamics also makes it intrinsically challenging to define their precise locations on the proteasome47,48”, do they mean that Rpn13 was not determined? Authors should provide details on these aspects.

2. Usp14 is an important associated subunit of the proteasome, with relevant allosteric regulation of the proteasome mechanism, influencing ubiquitin processing and affinity. Authors have excluded Usp14 in their approach, and they have not even mentioned Usp14 in the manuscript. Usp14 should be cited in the manuscript and an explanation of the reasons for not including Usp14 in the work should be provided.

3. The human 26Sproteasomes used in this work are purchased in UBPBio. It is quite surprising that such an important material for this work to be purchased and not prepared in-house. But it is acceptable. Nonetheless, given the importance of the item, it should be included in M&M the exact reference and a brief description of the method of purification used by the company, and the processing carried out in the lab (if it was directly used or somehow processed– aliquots, melting/freezing cycles, buffer changing, etc). This information is also crucial to make the assays replicable.

4. In the Cryo-EM data processing and model building section (in the main text and in the scheme in Supplementary Fig. 4), it is mentioned that initially, two pools of proteasomes were classified, singly capped (RP-CP) and doubly capped (RP2-CP). This section shows issues that should be solved:
-it is used up to six times the term “RP-CP2”, which is inexistent. The right term is RP2-CP
-the numbers of RP-CP and RP2-CP (575,778 and 527,610) are swapped in the text (or in Supplementary Fig. 4).

5. Moreover, authors mention that both RP complexes from RP2-CP complexes were pooled together for data refinement and processing. At this stage it would be highly informative to know how frequently RP2-CP contained the substrate in both RPs, which conformations prevailed and how did they statistically differ from single capped (RP-CP) proteasomes (if they did). In other words, it is a good opportunity to define if there’s any bias in substrate binding between the two RPs of RP2-CP complexes, and between RP2-CP and RP-CP, and if these groups represent statically different pools concerning substrate binding.

6. The structural description of the surfaces (Rpn2 groove and neighboring subunits) that accommodate K11/K48 branched ubiquitin branch is excellent and potentially highly relevant, constituting probably the strongest novelty of this study. Given the importance and the implications of the discovery, it is mandatory to ask as a reviewer (as mentioned above) about the functional validation of the interacting role of the Rpn2 groove (and other proximal surfaces) in binding the different ubiquitin groups of K11/K48 branched ubiquitin. The literature has put the focus of K11/K48 branched ubiquitin recognition on Rpn10 (Rape) and Rpn1 (Fushman). Therefore, the novel role of Rpn2, which is presented as an evolutionarily conserved element in Rpn2, would be highly reinforced with functional validation with a distinct approach. Did authors tested if proteasomes carrying mutations in the most relevant amino acid positions in Rpn2 (mainly E538 and D564, but likely additional proximal positions) show decreased degradation or bindning of the model substrate (or other substrates modified with K11/K48-branches)? Or alternatively, does the expression of a mutated version of Rpn2 in human cells generate a phenotype or any signature of deficiency in degradation? I am not asking for an extensive genetic analysis, but a minimal functional validation should be required. In the case case this data in not provided, authors should give detailed explanations to justify this absence.

7. The dissection of UbI , UbII, UbIII, and UbIV, interactions in the RP is really excellent. The dissertation and figures provided are very clear. Concerning UbIV and the positioning role of UbIII, in line 205: “Given the sparse contacts made by the K11-linked UbIII with RPN2, the primary role of UbIII appeared to restrict the conformational space available to UbIV for positioning it to the new Ub binding groove formed by RPN2 and RPN9.” Did authors analyse the position of equivalent UbIV in the complex containing K11-only substrate? How this UbIV and UbIII are accommodated? This is relevant since K11-chains are described in the literature and more abundant than branched forms. Furthermore, when branches are formed, it is expected that K11 linkage to be maintained in the growing branched chain, which is not the case of Sic1PY-Ubn(K63R) generated in this work. Could authors shed light to these issues?

8. In line 226, it is mentioned :“In contrast, in the ED:Ub4 state, the interaction network between the RPN2 and UbIV underwent rearrangements resulting in reduced intermolecular hydrogen bonds and salt bridges (Supplementary Table 1)”. However, in the following paragraph and in Supplementary Table 1 no decrease of salt bridges between UbIV and Rpn2 is shown. Moreover, the overall decrease of contacts is very mild. Could authors fix and argue this inconsistency?

Additional points:

1-Fig. 3 legend shows errors in panel labeling. “b” and “c” are swapped.

2-line 140, “Fig. 1e” should be “Fig. 1f”

3-line 173, “Fig.1d-f” should be “Fig. 1e-g”

4-line 268, “RPT11” should be “RPN11”

5-line 273, “PR” should be “RP”

6-line 305, “Walkers” should be corrected. “Walters” is the right name.

7-line 329, “Additional contacts made by RPN8, RPN9, and RPN10 may be necessary to generate sufficient multivalency (Fig. 2, Fig. 3a, and Supplementary Fig. 9 and 10).” I don’t understand why these figures are cited here.

8-line 338: “The plasmids pRSFduet_His-TEV-gsggs-Ub(WT), pRSFduet_His-TEV-gsggs-Ub(K0), pET21d_His-hE1, pETduet_His-SUMO-gg-UBCH7, pGEX_TEV-SENP2, pMBP_TEV-Rsp5-WW3-HECT, and pMBP_TEV-Rsp5 WW3-HECT_GML were synthesized by (GeneScript, USA).”
This sentence is not clear and it seems to be incomplete : what was synthesized by who?

9-line 358: wrong heading

7-line 796, “fffinity” should be fixed

8 -line 314, in the paragraph: “The conformational changes within the ATPase assembly were reminiscent of the previously reported activation mechanism of archaeal PAN ATPase52, and the activation mechanism of the ATPase unfoldase activity upon Ub binding to the proteasomal Ub receptors53.” In this context it would be good to reference Ding et al., 2019 (10.1016/j.molcel.2019.01.018) since it is a relevant work on the effect of tetraubiquitin on proteasome conformations.

9-in Supplementary Information (page 1), “Supplementary text” is mentioned in the index, but missing in the document. If there’s a whole “Supplementary text” missing, it needs to be revised.

10- Supplementary. Fig. 12 legend shows errors in panel labeling. “e” doesn’t exist, it should be “d”. “d” should be “c” . “b” and “c” should be corrected.

In general, the good correspondence of figures, panels in the text should be doublechecked.

Reviewer #2

(Remarks to the Author)
The authors reconstituted a functional 26S proteasome complex containing a specially engineered K11/K48-branched polyubiquitinated substrate and determined multiple cryo-EM structures that reveal how the proteasome recognizes such branched ubiquitin chains. Notably, they identified a previously uncharacterized, multi-subunit “groove” on the 19S regulatory particle—formed by RPN2, RPN8, RPN9, RPN10, and RPN11—that selectively accommodates the K11-linked branch, thus enhancing substrate affinity and driving the proteasome’s catalytic cycle.

The manuscript is logically structured and clearly written overall. The key findings are adequately supported by the presented data. However, the authors attempted to visualize the substrate and UCHL5 in the cryo-EM density maps, no density was apparent—likely due to the proteasome’s intrinsic dynamics. To further probe these interactions, crosslinking mass spectrometry (MS) was employed, but concerns about the design and execution of the crosslinking experiments limit the reliability of those particular findings.

Meanwhile, the crosslinking MS community has established robust and continually evolving protocols for public data deposition. Following the reporting standards outlined in “Toward Increased Reliability, Transparency, and Accessibility in Cross-linking Mass Spectrometry” (PMID: 33065067), I strongly encourage the authors to deposit the crosslinking MS datasets in PRIDE/ProteomeXchange to ensure transparency and reproducibility.

Comments and concerns:

The groove surrounded by RPN2, RPN11, and RPN10 has recently been reported as a binding site for the PITH domain as well. (bioRxiv https://doi.org/10.1101/2024.11.08.622741, https://doi.org/10.1101/2024.12.04.626795, https://doi.org/10.1101/2024.11.08.622731)
Could you discuss it and support the biological impact of your finding?

(Line 689)
The authors indicate that the functional 26S proteasome complex used for XL-MS was prepared “in the same way as for the cryo-EM experiment.” However, ATP—containing a primary amine—can quench NHS-ester crosslinkers, and β-mercaptoethanol (βME) further disrupts crosslinking reactions. Consequently, these conditions likely explain why crosslinks between the proteins of interest were barely detectable, and why almost no crosslinks were observed among the proteasome subunits.

Why did the authors use only 0.08mM DSSO?

Have you verified the effectiveness of the DSSO crosslinking reaction by running an SDS-PAGE gel or Western blot post-crosslinking? It would be helpful to include the corresponding Coomassie-stained gel or Western blot figure in the supplement.

I also recommend performing a titration of the DSSO crosslinker to confirm optimal crosslinking conditions. Even if the crosslinking is carried out successfully, offline peptide fractionation is strongly advised before LC-MS analysis. This step helps remove shorter (or less-charged) linear peptides, thereby enhancing the identification and detection of crosslinked peptides.

(Line 711)
The authors report that MS1 and MS2 scans were acquired in the Orbitrap at resolutions of 60,000 and 30,000, respectively, while MS3 scans were acquired in the ion trap.

Could you clarify why lower resolutions were chosen in these experiments?

I suggest that the authors move to more simple MS2 methods - they give a more reliable FDR, and they are easier for a simple sample like a single complex. https://www.nature.com/articles/s41467-022-31701-w

(Supplementary Fig. 6.)
It is currently very difficult to draw concrete conclusions about the interaction network derived from the XL-MS analysis. I recommend addressing the following points:
1. Residue Pairs: Could you please provide the specific residue pairs for key crosslinks shown in the network? Additionally, the corresponding MS spectra for the key crosslinks should be included to support your conclusions.
2. Origin of Ubiquitin: Where does the ubiquitin (Ub) depicted in Supplementary Fig. 6(a) originate?
3. RPN1–Ub Crosslinks: Can you explain why no crosslinking was observed between RPN1 and Ub?
4. Validation with Known Structures: Have you verified that the identified crosslinks (e.g., UCHL5–RPN13, UCHL5–Ub) align with known structural information?
5. RPN3–Ub Interaction: RPN3 is unlikely to interact with Ub. Do you have any hypothesis or explanation for this unexpected result?
Addressing these questions and clarifying the data would help strengthen the conclusions drawn from Supplementary Fig. 6.

Minor:

(Line 305) “Walkers” needs to be changed to “Walters”.

Reviewer #3

(Remarks to the Author)
This paper describes a single particle cryo-EM based investigation into the mode of binding of a K11/K48-branched tetra ubiquitin chain to the human 26S proteasome. Understanding the structural basis of branched ubiquitin chain recognition by the proteasome is an important matter both with respect to the biology of the system and its potential in drug development. The major problem with the paper as currently presented is the limited resolution of the analysis, particularly in the part of the structure that is most important for this study – the tetraubiquitin chain and its immediate environment. The authors claim to identify each of the ubiquitin molecules as well as the linkage in their cryo-EM map. Ubiquitin chains are assembled by linking the extended single stranded C-terminal tail of one ubiquitin to an amino group (in this case that on the side chain of lysine 11 or lysine 48) on the subsequent ubiquitin molecule. The authors state “Importantly, we unambiguously resolved the cryo-EM densities of a K11/K48-branched tetra-Ub(Ub4) chain bound to the EB and ED states (hereafter EB:Ub4 and ED:Ub4, respectively;)” referring to Figure 1 d-f (here I think they mean Figure 1 e-g) and their supplementary movie.
In my opinion the figure and movie do not unambiguously support their model. Ideally, to do this they should be able to unambiguously trace the complete chains of each ubiquitin and its linkage within their density maps. This does not appear to be the case. In Figure 1 e & f they identify a set of 4 densities which they ascribe to ubiquitin. Although these densities are generally consistent with ubiquitin, the level of detail does not appear sufficient to identify secondary structure detail and hence it is not clear that the ubiquitin molecules have been docked in the correct orientation. For some reason, more detail is shown in Figure 1g. Nevertheless, the densities ascribed to ubiquitin still appear to lack secondary structure detail and the match between the map and fitted models is incomplete with regions of model such as the C-terminal tail of ubiquitin IV falling outside the experimental density and regions of experimental density which are not explained by the model.
In the light of the above comments I recommend that the authors revise their interpretation of the ubiquitin density assignments. It is possible that a detailed consideration of possible docking geometries and agreement with their experimental maps may allow them to identify a unique solution and rule out alternatives. If this could be argued in a convincing and logical fashion I would find the paper acceptable for publication.

Version 1:

Reviewer comments:

Reviewer #1

(Remarks to the Author)
In the new version of the manuscript, authors have made an extraordinary effort and answered all the questions raised in the first version.

I have to acknowledge the great improvement of the work.

I am also glad that my suggestions have been positively used in the current manuscript.

In my view, this is an outstanding work and it will be of interest for a broad audience. Therefore, I strongly recommend this manuscript for publication in nature communications.

Reviewer #2

(Remarks to the Author)
The authors have addressed my substantive concerns, and I support publication in Nature Communications.

I have a few minor comments below.

Reviewer credentials for the PRIDE dataset were not provided.

The revision appears to use an updated version of the analysis software (with fixes to FDR estimation and other bugs) that substantially improves the results relative to the original submission. However, several aspects of the experimental workflow remain unclear and may be suboptimal. Analyzing the 26S proteasome by SDS-PAGE or Western blot after crosslinking is feasible; if practical, please include a gel-based comparison of crosslinked and non-crosslinked samples (Western blot or stained gel). While optional, this addition would strengthen the manuscript.

Given reports that DSSO can yield elevated false-positive rates, it would strengthen the manuscript to include a figure mapping all identified crosslinks onto a high-resolution proteasome structure and to quantify overall reliability (e.g., the fraction of inter-subunit crosslinks across all proteasome subunits that satisfy expected distance constraints). This would be more informative than emphasizing the over-length crosslinks between RPN3 and the ubiquitin chain (Supplementary Fig. 10d).

Reviewer #3

(Remarks to the Author)
The authors have made a number of revisions to their manuscript and go some way to addressing my concerns about their interpretation of the densities they assign to the Ub4 molecule with their new supplementary figures. However, I remain concerned that the main text is still misleading with respect to the confidence with which they make their assignments. They continue to state that their interpretation derives from their ability to “unambiguously resolve the cryo-EM densities of a K11/K48-branched tetra-Ub (Ub4)”. In my view the interpretation of their cryo-EM densities is far from unambiguous. They place considerable confidence in their assignment of individual densities to the extended C-terminal ubiquitin tails. Given that individual strands are not resolved in the beta-sheet regions of ubiquitin densities (supplementary fig R7), it is not clear that the details of the EM densities they assign to the ubiquitin C-terminal tails can be relied on. This can be appreciated by considering the various panels of supplementary figure R7 in which the threshold chosen to maximise visibility of secondary structure elements within the globular domain ubiquitin domains leads to fragmented density for the C-terminal tails.

It would be better if the authors were to acknowledge that in this matter they are working close to the limits of resolution and signal to noise ratio. They would probably be justified in putting forward their model as being the most likely interpretation (comapred to alternatives) based on the various arguments presented in their new supplementary data, but I think they should explicitly make this argument in an objective fashion rather than claiming that each new observation confirms their original conclusion.

Point-by-point responses to the reviewers' comments

We appreciated the reviewers' constructive comments that help improve our manuscript. Please find below the point-by-point responses to the reviewers' individual comments. The corresponding changes in the revised manuscript are highlighted in blue.

Reviewer #1 (Remarks to the Author):

In this manuscript, Draczkowski and colleagues present a cryo-EM study of human 26S proteasome associated with a model ubiquitinated substrate. The authors engineer the process of in vitro ubiquitination in order to generate the substrate modified with K11/K48-branched ubiquitin chains, a type of heterotypic chain with reported enhanced degradation and affinity towards the proteasome, and a partially characterised mode of interaction with proteasomal ubiquitin receptors. With this approach, the authors obtain multiple conformational variants of the 26S – substrate complex with a very good definition of up to four ubiquitin molecules defining the K11/K48-branch, and uncover and nicely describe a putative novel K11/K48-branched ubiquitin interaction region, based on a conserved motif in Rpn2 subunit and on multiple adjacent surfaces of neighbor subunits.

One notorious experimental paradox in the field is that, in a context of deficiency in the described (and well-characterised) proteasomal ubiquitin receptors (RPN10 [UIM], RPN13 [PRU] and RPN1 [T1]), and in the absence of substrate UBL-UBA shuttles, 26S proteasomes are still capable to degrade ubiquitinated substrates. Based on that, it has been hypothesised that at least one additional ubiquitin-binding surface must be hidden in the regulatory particle of the 26S. In this work, the authors claim having discovered this cryptic ubiquitin recognition site, which appears to be sculpted to bind K11/K48-branched Ub species.

Furthermore, the work is rich in detailed data which describe important additional aspects that help to comprehend the interaction of distinct ubiquitin moieties of polyubiquitinated proteins with the subunits of the RP of the proteasome.

Overall, the work is very well designed and the data presented is outstanding, with profound analysis and discussion. Referenced bibliography is fine (however some suggestions are added).

Said that, since the work is focused on a unique approach, without additional functional validations of the discoveries (for example, mutations of key positions), the current version is placed in the borderline of acceptance in Nat Comms, from the stand point of this reviewer. The feeling is that the high quality of the data could make this work acceptable after addressing the following issues (which could be defined as "minor")

Main issues that should be addressed are:

1. The experimental approach includes a well-designed plan to integrate Rpn13 and inactive UCHL5(C88A) in the whole reconstituted 26S-Sic1PY-Ubn(K63R)-UCHL5(C88A) complex. However, the reconstitution evidence shown (Supplementary Fig. 2) are not clear and panels

have some problems. Panel A shows native gels cut. It is important to know whether the lanes correspond to the same electrophoresis run, otherwise it's impossible to know that the shift is real. In panel B, it is not shown a Rpn13 western blot. Did proteasomes before reconstitution contain endogenous Rpn13 and UCHL5? It is also puzzling that the RP-CP show no WB signal for Ub and UCHL5, Do authors have an explanation for that?

We want to thank the Reviewer for pointing out the unclear description of the sample composition. We decided to supplement the human 26S proteasome sample preparation with an excess of RPN13:UCHL5(C88A) for several reasons.

Deol *et al*., 2020, and Song *et al*., 2021 (ref. 21, 22 in the manuscript) showed that UCHL5 preferentially cleaves K48-containing branched chains and that RPN13 is important for its debranching activity. Therefore, we added the preformed RPN13-UCHL5(C88A) complex to the 26S proteasome sample, hoping that in the presence of the substrate with K11/K48-branched Ub chains ($Sic1^{PY}$-Ub_n(K63R)), the conformational dynamics of the proteasome-bound UCHL5 would be reduced, allowing us to map the enzyme's position on the functional 26S complex, which to date remains unknown despite multiple reported structures of the human proteasome. Before the structural analysis, we performed extensive quality checks of the 26S proteasome sample used in the study, including Western blot analysis, activity assays, and mass spectrometry protein ID assignments. The analysis revealed that the 26S proteasome sample already contained a sub-stoichiometric amount of endogenous co-purified UCHL5 (**Figure R1**). We were able to increase the amount of proteasome-bound UCHL5 by supplementing the sample with the purified recombinant RPN13-UCHL5(C88A) complex. By adding excessive amounts of catalytically dead UCHL5(C88A), we aimed to competitively replace the wild-type endogenous UCHL5 on the proteasome complexes with the inactive version of the enzyme to prevent cleavage of the proteasome-bound Ub chains before the vitrification of the cryo-EM grids.

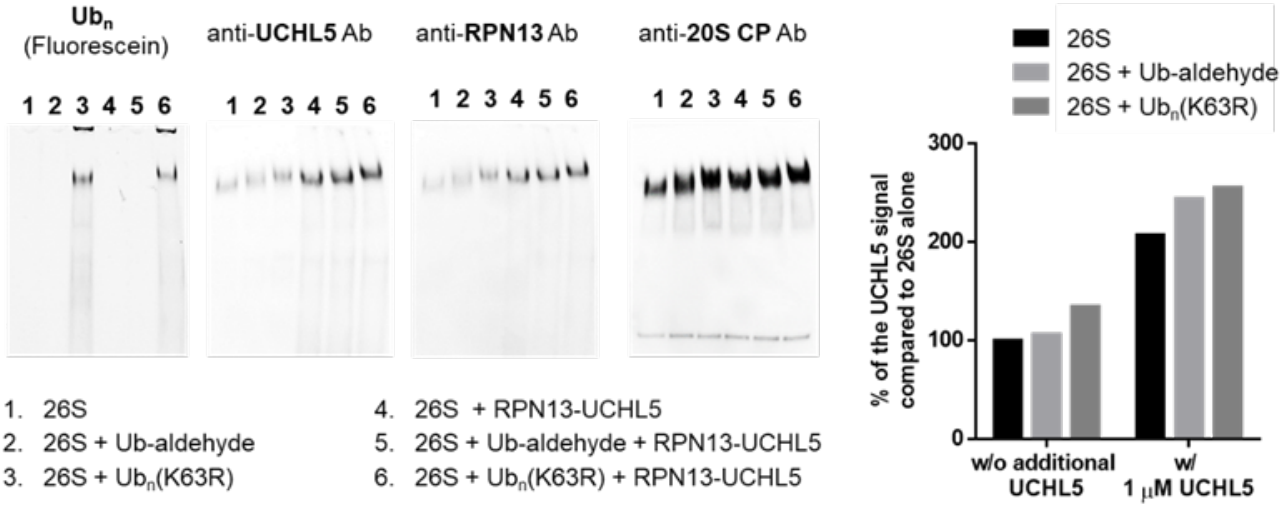

Figure R1. Western blot analysis of the 26S complexes, both in the absence and presence of Ub. *The quantification of UCHL5 (bar plot) indicates an enrichment of proteasome-bound UCHL5 when the sample was supplemented with an excess of recombinant RPN13-UCHL5 complex.*

We also observed that increasing the amount of UCHL5 bound to the proteasome enhanced the substrate binding by the 26S complex. This was confirmed through immunodetection and by monitoring fluorescent signals mounted on the substrate (**Figures R2**).

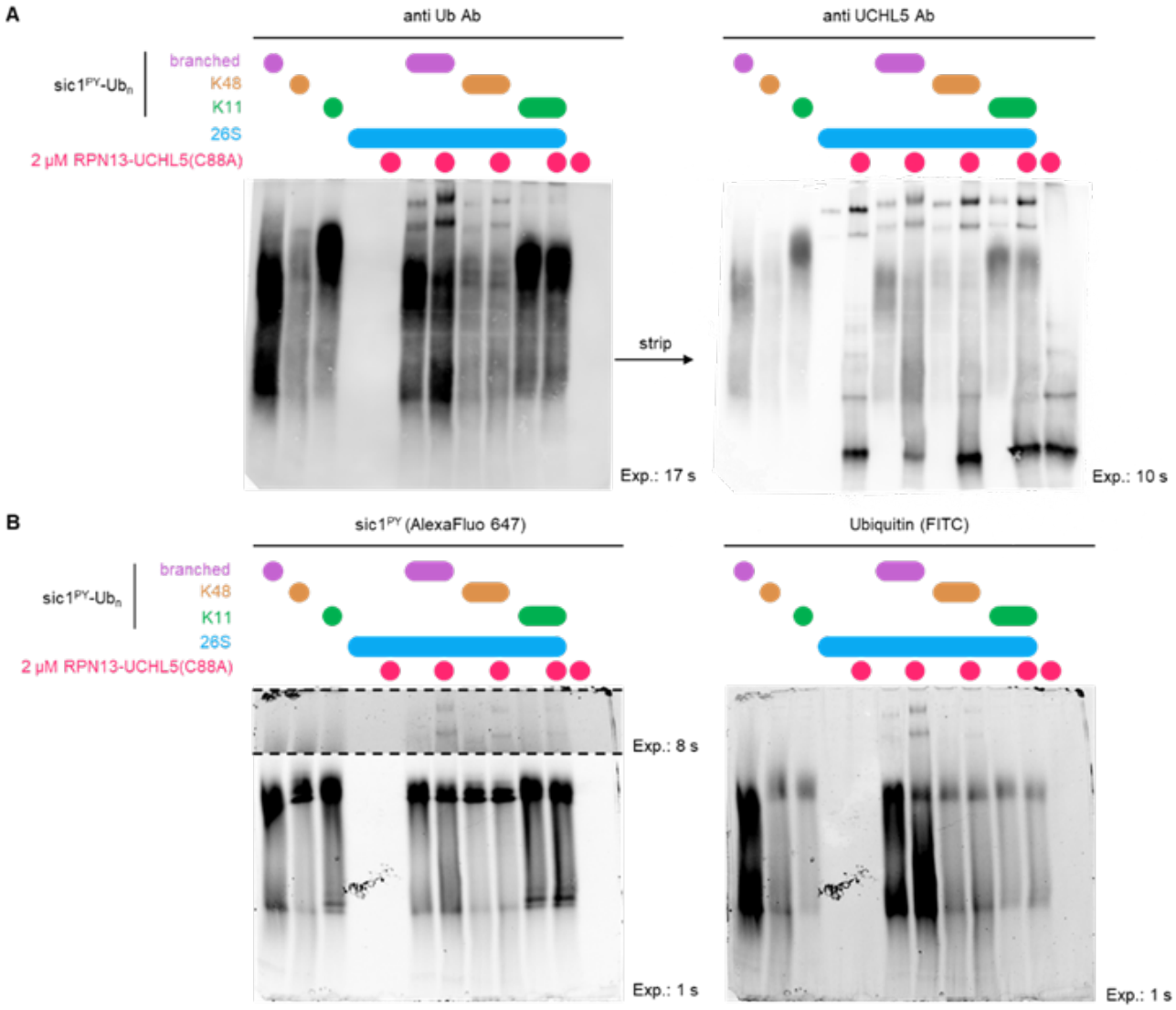

Figure R2. Native gel analysis of the effect of substrates tagged with various Ub chains and UCHL5(C88A) on their binding with the 26S proteasome. *Results indicate an increase in proteasome-bound UCHL5 in the presence of the substrate, especially when the complex was supplemented with the preformed RP13-UCHL5(C88A) complex. The addition of recombinant RPN13-UCHL5(C88A) also significantly increased the binding of Sic1^{PY}-Ub$_n$(K63R) to the proteasome.*

We evaluated the effect of excess UCHL5 on substrate processing by the 26S proteasomal complex (**Figure R3**). By quantifying the fluorescent signal of the Sic1^{PY} degradation products at various time points, we found that the addition of the catalytically inactive RPN13-UCHL5(C88A) complex enhances the proteolysis of the substrate modified by K11/K48-branched Ub chains, but not by K11-only or K48-only Ub chains.

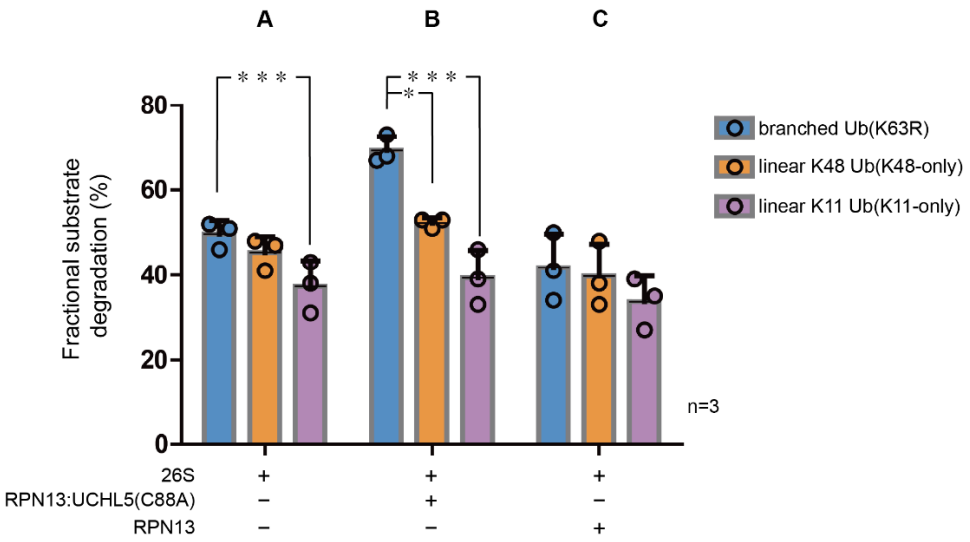

Figure R3. Effect of UCHL5 on proteasome-mediated substrate degradation marked by branched or linear Ub chains. *UCHL5's deubiquitinating activity was shown to play a regulatory role in the degradation of Sic1^{PY} marked with branched Ub chains. The fraction of the substrate marked with branched (blue bars) and linear K48-linked (orange bars) Ub chains that was degraded by the 26S complex containing endogenous UCHL5 was comparable (A). However, substituting the wild-type enzyme with an excess amount of catalytically inactive UCHL5(C88A) mutant resulted in significantly enhanced degradation of Sic1^{PY} tagged with branched chains compared to those marked with linear Ub chains (B). (C) Adding RPN13 alone did not reproduce the outcome, confirming that the effect was solely due to UCHL5. Regardless of the complex composition, the linear K11-linked Ub chains (purple) proved less efficient in targeting the substrate for degradation.*

Supplementary Fig. 2B shows the results of one of the Native gels > Western Blot analyses, where we confirmed the binding of the RPN13-UCHL5(C88A) to the 26S proteasomal complexes. We cut the gel in this panel and the gels shown in panel A of the same figure to facilitate interpretation, since we usually run native gels with as many samples as possible to optimize reagent consumption. As requested by the Reviewer, we present the uncut gels in **Figure R4**.

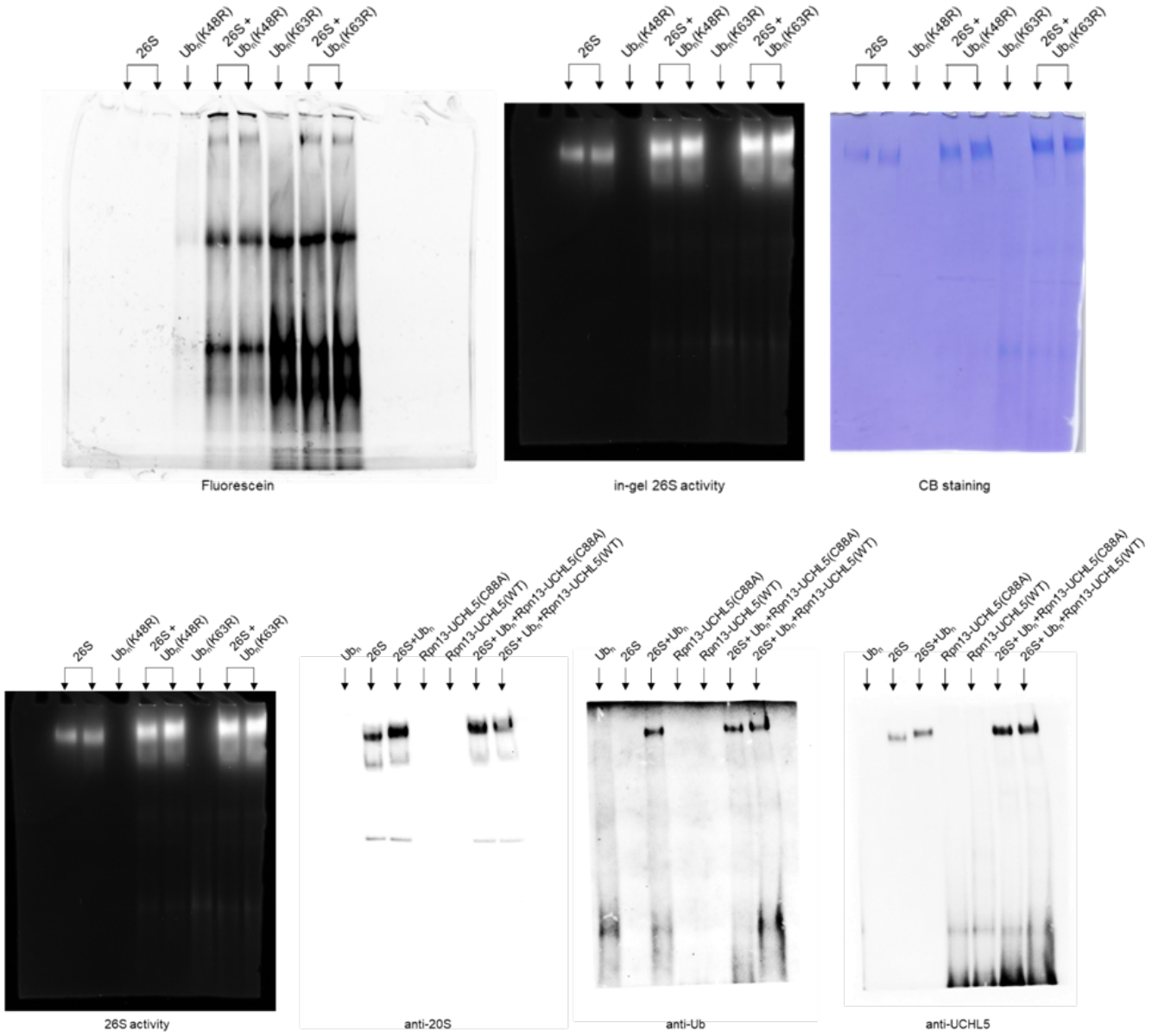

***Figure R4**. Uncut version of the native gels presented in Supplementary Fig.2.*

We detected WB signals for Ub and UCHL5 on both RP2-CP and RP-CP complexes. However, the intensity of the signals was low in the band corresponding to the RP-CP. Consequently, visualization of RPN13 and UCHL5 in the band corresponding to RP-CP required longer exposures, which resulted in oversaturation of the signal in the RP2-CP band. We decided to stay within the dynamic range of the gel imager and captured the final images at a lower exposure time. We agree with the Reviewer that the low signal for Ub and UCHL5 at the RP-CP is intriguing, but we believe this is due to the overall low amounts of RP-CP in this particular sample. Later, we noticed that pre-warming of the thawed 26S sample may affect the reassembly of the complex. For the structural experiments, the complex was incubated at 37

°C before and after the addition of the other components, as described in the Materials and Methods section of the manuscript.

Additionally, UCHL5 could not be resolved in the EM structures obtained (this point is discussed by authors), but nothing is mentioned about Rpn13. Could Rpn13 be resolved? When authors mention that (line 149): "Nonetheless, such functional dynamics also makes it intrinsically challenging to define their precise locations on the proteasome47,48", do they mean that Rpn13 was not determined? Authors should provide details on these aspects.

We appreciate the reviewer comment for further clarification about the resolvability of RNP13 on the 26S proteasome in our cryo-EM investigation. Despite confirming the presence of both RPN13 and UCHL5 in the reconstituted proteasome complexes, we still could not resolve them in the cryo-EM map of the complex, even with the substrate present. As discussed in the manuscript, we assume that UCHL5 binds to the distal parts of the proteasome-bound Ub chain (including other branching points that may exist along the Ub chain). The high dynamics of UCHL5 and the RPN13 DEUBAD domain presumably allow the system to adapt to a wide range of structurally diverse proteasome substrates. We also did not observe a well-defined density for the PRU domain of RPN13, which directly binds to the proteasome. We attribute this to the RPN13 PRU binding to the flexible C-terminus of RPN2, which also provides a considerable degree of conformational freedom. Independently, we used cross-link mass spectrometry (XL-MS) to identify multiple (transient) interactions of RPN13 with RPN2, RPN10 and the core particle subunits PSA3 (α3) and PSB7-2 (β7) – see our response to Reviewer #2's comment below. The intrinsic dynamics of UCHL5, RPN13 and RPN2 pose a challenge for cryo-EM reconstruction, as they blur out when averaging thousands of particle cryo-EM images. For these reasons, none of the human proteasome structures reported to date have resolved the density of the proteasome-bound UCHL5 or RPN13/ADRM1.

To clarify the description of the unresolved parts of the complex, we modified the sentence (line 160) in the manuscript that reads:

"*Despite the addition of an excess amount of UCHL5(C88A), we did not observe EM density that could be assigned to RPN13-bound UCHL5 in any of the four functional states*."

To:

"*Despite the addition of an excess amount of UCHL5(C88A), we did not observe EM density that could be assigned to RPN13-bound UCHL5 nor the DEUBAD/PRU domains of RPN13 in any of the four functional states."*

2. Usp14 is an important associated subunit of the proteasome, with relevant allosteric regulation of the proteasome mechanism, influencing ubiquitin processing and affinity. Authors have excluded Usp14 in their approach, and they have not even mentioned Usp14 in the manuscript. Usp14 should be cited in the manuscript and an explanation of the reasons for not including Usp14 in the work should be provided.

Usp14 and UCHL5 are responsible for trimming proteasome-bound Ub chains; therefore, both are important for substrate processing by the proteasomal complex. However, it has been shown that the substrate specificity of Usp14 and UCHL5 differs. While UCHL5 exhibits K48-linkage-specific debranching activity (ref. 21, 22 in the manuscript), Usp14 (or Ubp6 in yeast) is

proposed to be mainly K63-linkage specific (PMID: 25389291; PMID: 25575639) or to catalyze the removal of supernumerary ubiquitin chains on a substrate *en bloc* (ref. 30 in the manuscript). More importantly, the structural basis of how Usp14 interacts with the 26S proteasome has been extensively investigated by Mao and colleagues in their 2022 Nature paper (ref. 46 in the manuscript). Therefore, we decided to focus on UCHL5, as it appears more relevant in the context of branched Ub chain processing by the proteasome. Nonetheless, we agree with the reviewer that the role of Usp14 in Ub chain processing by the 26S proteasome is worth mentioning in the manuscript, along with an explanation of why Usp14 was not included in the studied complex. Therefore, we added the following text to the manuscript (line 66):

"*Apart from UCHL5, the proteasome can reversibly bind to another auxiliary DUB, USP14. Several cryo-EM studies have revealed the molecular basis of USP14 (or its yeast homolog Usp6) in the context of proteasome functions*[23-27]*. Unlike UCHL5, which exhibits K48-linkage-specific debranching activity, USP14 is proposed to be mainly K63-linkage specific*[28,29] *or to catalyze the removal of supernumerary ubiquitin chains on a substrate en bloc*[30]."

We hope the reviewer will find these additions sufficient.

3. The human 26S proteasomes used in this work are purchased in UBPBio. It is quite surprising that such an important material for this work to be purchased and not prepared in-house. But it is acceptable. Nonetheless, given the importance of the item, it should be included in M&M the exact reference and a brief description of the method of purification used by the company, and the processing carried out in the lab (if it was directly used or somehow processed– aliquots, melting/freezing cycles, buffer changing, etc). This information is also crucial to make the assays replicable.

We agree with the reviewer that a clear description about the sample preparation is important for the reproducibility of our work. We have contacted UBPBio for more clarification on the sample preparation procedure and the response was as follows:

"*UBPBio offers the human 26S proteasome (Catalog No.: A1100 and A1101), sourced from HEK 293 cells. The complex was purified following method published by Wang et al. (*ref. 68 in the manuscript*), with modifications. According to the reported method, the human 26s proteasome was isolated from a stable HEK 293 cell line expressing the Rpn11 subunit with an HP affinity tag for the complex purification.*"

Regarding the quality of the commercial 26S proteasome sample, the UBPBio in the product specification sheet for the human 26S proteasome states that the preparation is characterized by >90% purity according to Native-PAGE, which is supported by Coomassie-stained SDS-PAGE analysis of the product. Those results were consistent with our quality checks of the received sample. In addition to the analysis provided by the company, we also conducted a spectrophotometric activity assay using Suc-LLVY-AMC substrate to assess proteasome activity. We evaluated the stability of the preparation by measuring its proteolytic activity after freeze-thaw cycles and at 4°C in different buffers. Additionally, we assessed the proteasome composition using mass spectrometry protein ID analysis, which confirmed the presence of the

26S complex's constitutive components, as well as co-purified endogenous RPN13 and UCHL5 (see the XL-MS part below). Finally, we collected a cryo-EM dataset with the "apo" 26 proteasomes to confirm that the commercial preparation is suitable for structural analysis. This dataset produced a 3.2 Å resolution map of the resting-state proteasome **(Figure R5**) that did not show any significant additional densities apart from those contributed by the constitutive proteasomal subunits.

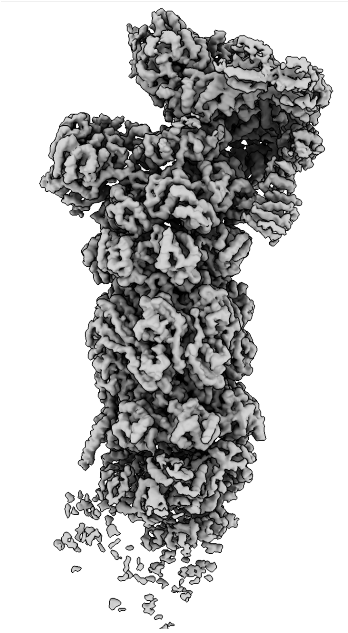

Figure R5. The 3.2 Å resolution map of the human 26S proteasome complex sourced from UBPBio*. The map represented the resting state structure consistent with those reported in the literature, without any obvious additional densities that would correspond to proteasome-interacting proteins or substrate*.

After these QC and optimization steps, we requested UBPBio to tailor make a large batch of the 26S proteasome stored in HEPES buffer instead of TRIS buffer, the standard buffer used by UBPBio for shipping the complex at that time. Although we could not obtain further details regarding the procedures of purifying the 26S proteasome by UBPBio, we felt that we had done sufficient controls to ensure the quality and purity of the proteasome for further structural and functional investigations in this study. To address the reviewer's comment, we added the following text to the Materials and Methods section of the manuscript along with the corresponding reference.

"*The human 26S proteasome complex used in the study was purchased from UBPBio, USA (Catalog No.: A1100 and A1101). The complex was expressed in human HEK 293 and affinity purified following the procedure described by Wang et al* (ref. 68 in the manuscript*), with manufacture modifications. The proteasome sample was custom-made to be stored in HEPES buffer as frozen aliquots, shipped on dry ice and stored at -80 ºC before use. The aliquots were thawed immediately before use. The purity of the sample was confirmed by native and*

SDS-PAGE; the activity of the sample was confirmed using a Suc-LLVY-AMC substrate followed by spectrometric analysis."

We hope the reviewer will find these additions satisfying.

4. In the Cryo-EM data processing and model building section (in the main text and in the scheme in Supplementary Fig. 4), it is mentioned that initially, two pools of proteasomes were classified, singly capped (RP-CP) and doubly capped (RP2-CP). This section shows issues that should be solved:
-it is used up to six times the term "RP-CP2", which is inexistent. The right term is RP2-CP
-the numbers of RP-CP and RP2-CP (575,778 and 527,610) are swapped in the text (or in Supplementary Fig. 4).

We thank the reviewer for pointing out this typo that regrettably made it into the manuscript. The RP-CP and RP_2-CP notations have been corrected across the entire manuscript.

5. Moreover, authors mention that both RP complexes from RP2-CP complexes were pooled together for data refinement and processing. At this stage, it would be highly informative to know how frequently RP2-CP contained the substrate in both RPs, which conformations prevailed, and how they statistically differed from single-capped (RP-CP) proteasomes (if they did). In other words, it is a good opportunity to define if there's any bias in substrate binding between the two RPs of RP2-CP complexes, and between RP2-CP and RP-CP, and if these groups represent statically different pools concerning substrate binding.

We want to thank the Reviewer for raising this interesting question. Indeed, the fact that we were able to resolve the clear density of the tetra-ubiquitin bound at the RP subcomplex of the human proteasome provides an opportunity to evaluate any preference for substrate binding by the RP_2-CP or RP complexes. The reported dataset also allows for examining any potential cooperativity or correlation in the conformations adopted by the two RPs in the RP_2-CP complexes.

It is worth noting that obtaining high-resolution cryo-EM structures of such a complex system requires meticulous classification and filtering of the particle image sets to discard low-quality images collected on grid areas with suboptimal ice, which may suffer from imaging artefacts or partially denature due to contact with the air- water interface. This stringent filtering procedure may skew the number of particles in each observed population. Therefore, the statistics of the conformational states, *i.e.*, the relative populations of the substrate-engaged states of the RP_2-CP, may not represent the true populations under native conditions. Nevertheless, inspired by the reviewer's suggestion to explore the question further, we endeavored to explore the aspects in further details.

Instead of the final particle stacks for analysis, we used the particle stacks from the early steps of data processing, representing 575,778 RP_2-CP and 527,610 RP-CP particles. We subsequently ran focused 3D classification (without further refinement of the particle alignment and with the regularization parameter T = 64) on each of the RPs in the RP_2-CP complex and conducted a similar classification focused on the RP of the RP-CP particles. Using an in-house script and the pySankey (https://github. com/anazalea/pysankey), we plotted the correlation

between the particles in each of the classes representing different conformations of the opposing RPs in the RP_2-CP complex. The results showed that in most of the RP_2-CP particles (82% of the analyzed), at least one RP existed in an active, substrate-processing conformation (added as a new **Supplementary Fig. 8)**. The reciprocal analysis of classes representing the two RPs showed that in most of the particles, if one RP is in the active conformation, then the RP on the opposite side of the RP2-CP complex (RP') is in a resting conformation; however, there were ~12% of particles in which both RPs were found bound with the Ub chain and adopted an active conformation, which was a surprise to us. Classification of the RP of the RP-CP particles showed that they adopt an active conformation less frequently (only 19% of the analyzed), compared to the RP_2-CP complex, suggesting that the engagement of the second RP to the CP may shift the population of the RP towards the active state (**Supplementary Fig. 8b)**. Note that in 36% of the RP-CP particles, the RP conformation could not be unambiguously assigned due to the low quality of the resulting 3D class volumes. This can be due to the poor quality of those particle images or errors in the initial particle alignments that propagated to the resulting 3D class volumes. We have added a paragraph on page 4 as follows to address this finding:

"The identification of substrate-free and Ub chain-bound 26S complexes in various conformational states allowed for the assessment of any preference for substrate binding by the RP_2-CP or RP complexes, as well as the examination of the cooperativity between opposing RPs within the RP_2-CP. Classifications focusing on the 19S RP subcomplexes showed that in the majority of RP_2-CP complexes (82% of those analyzed), at least one RP was found in an active (E_D-like) substrate-processing conformation (Supplementary Fig. 8). On the other hand, only 19% of the analyzed RP-CP particles exhibited the 19S RP in an active conformation. Reciprocal analysis of classes representing the two 19S RPs in the RP_2-CP complexes indicated that, generally, if one RP adopted the active conformation, the RP on the opposite side of the RP_2-CP complex (RP') adopted a resting (E_A- or E_B-like) conformation. Additionally, approximately 12% of the RP_2-CP particles were identified in which both RPs were bound with the Ub chain and adopted an active conformation. It should be noted, however, that the stringent filtering of the particle image sets involved in the cryo-EM single particle reconstruction may affect the number of particles in each observed population; therefore, this analysis may not the full representation of the true conformational landscape of the complex proteasome under native conditions."

We are very excited by this finding and feel that it would be useful information for the community. Therefore, we have included the results in the new Supplementary Fig. 8 in the revised manuscript with the procedure of particle classification in the Materials and Methods section (page 17).

Once again, we would like to thank the reviewer for the suggestion to carry this analysis, which indeed leads to new insights into the functional interplay between the two RPs on the same CP.

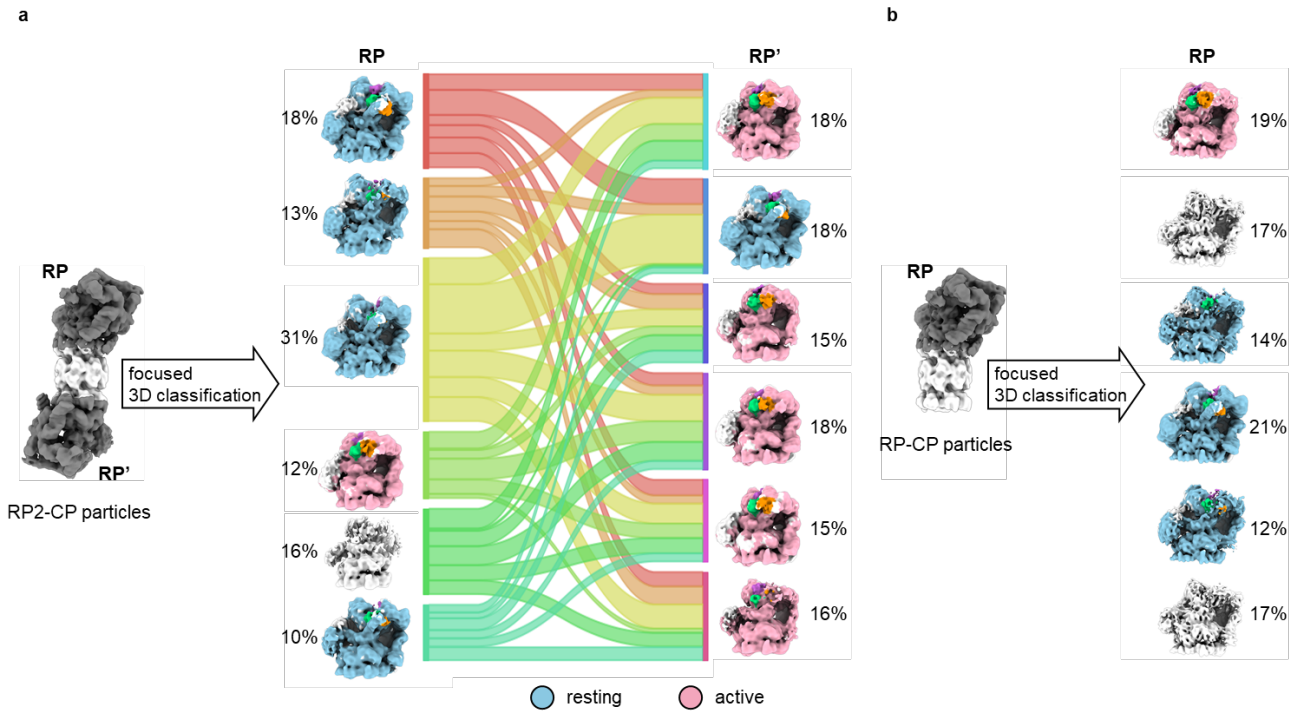

Supplementary Fig 8. Analysis of the substrate occupancy and conformations adopted by the regulatory particle (RP) on double- (RP2-CP) and single-capped (RP-CP) 26 proteasome complexes. *(**a**) 3D classes representing conformations adopted by the opposite RPs (RP and RP') of the RP2-CP particles, and the fraction of particles in each class (in percentages). The data-flow Sankey chart illustrates the results of reciprocal analysis of the RP and RP' classes, showing the connection between the conformations and functional states – resting (blue) and active (pink) – adopted by the opposite RPs. (**b**) Analogous 3D classification results performed on the RP subcomplex of the RP-CP particles.*

6. The structural description of the surfaces (Rpn2 groove and neighboring subunits) that accommodate K11/K48 branched ubiquitin branch is excellent and potentially highly relevant, constituting probably the strongest novelty of this study. Given the importance and the implications of the discovery, it is mandatory to ask as a reviewer (as mentioned above) about the functional validation of the interacting role of the Rpn2 groove (and other proximal surfaces) in binding the different ubiquitin groups of K11/K48 branched ubiquitin. The literature has put the focus of K11/K48 branched ubiquitin recognition on Rpn10 (Rape) and Rpn1 (Fushman). Therefore, the novel role of Rpn2, which is presented as an evolutionarily conserved element in Rpn2, would be highly reinforced with functional validation with a distinct approach. Did authors tested if proteasomes carrying mutations in the most relevant amino acid positions in Rpn2 (mainly E538 and D564, but likely additional proximal positions) show decreased degradation or bindning of the model substrate (or other substrates modified with K11/K48-branches)? Or alternatively, does the expression of a mutated version of Rpn2 in human cells generate a phenotype or any signature of deficiency in degradation? I am not asking for an extensive genetic analysis, but a minimal functional validation should be required. In the case this data in not provided, authors should give detailed explanations to justify this absence.

We appreciate the reviewer's suggestion and agree that functional validation is important. To address this point, we performed CRISPR-Cas9-mediated knockout (KO) of *PSMD1* gene (encoding RPN2) in HEK293T cells, which harbor three copies of the *PSMD1* gene. We electroporated HEK293T cells with Cas9 ribonucleoproteins carrying the *PSMD1*-targeting sgRNA. Initial analysis of the edited cells revealed ~70% KO efficiency at day 3 post-electroporation; however, this decreased to ~30% by day 7. The decline in KO efficiency over time suggests that *PSMD1* gene is essential for cell growth and that cells with complete *PSMD1* disruption are selected against. To further test this, we performed single-cell sorting in attempt to isolate homozygous *PSMD1* KO clones. However, all the surviving clones are confirmed by Sanger sequencing to be heterozygous and retained at least one intact *PSMD1* allele, indicating that complete Rpn2 loss is not tolerated in HEK293T cells.

In parallel, we performed CRISPR-mediated gene knock-in (KI) to introduce double mutations (E538A/D564A; designated as 2X KI) at the endogenous *PSMD1* locus. We employed a GFP-reporter-based selection system and enriched successfully edited cells through three rounds of fluorescence-activated cell sorting. We then compared the proliferation of parental and mutant cells using xCELLigence Real-Time Cell Analysis, which continuously measures cell density via electrical impedance. The 2X KI cell line exhibited reduced proliferation relative to WT KI in the first 48 hours post seeding. The instrument also measures cell death and detachment when the nutrients are depleted in the culture medium. In this context, the KO cells exhibited a delayed detachment relative to the parental cells; likewise, the 2X KI cell also exhibited a delayed detachment relative to WT KI, consistent with the expectation that a slower cell proliferation rate is accompanied by a slower depletion of the cell culture medium nutrients. The gene-editing design, sequencing results and cell proliferation results are included in the **Supplementary Fig. 16** as follows:

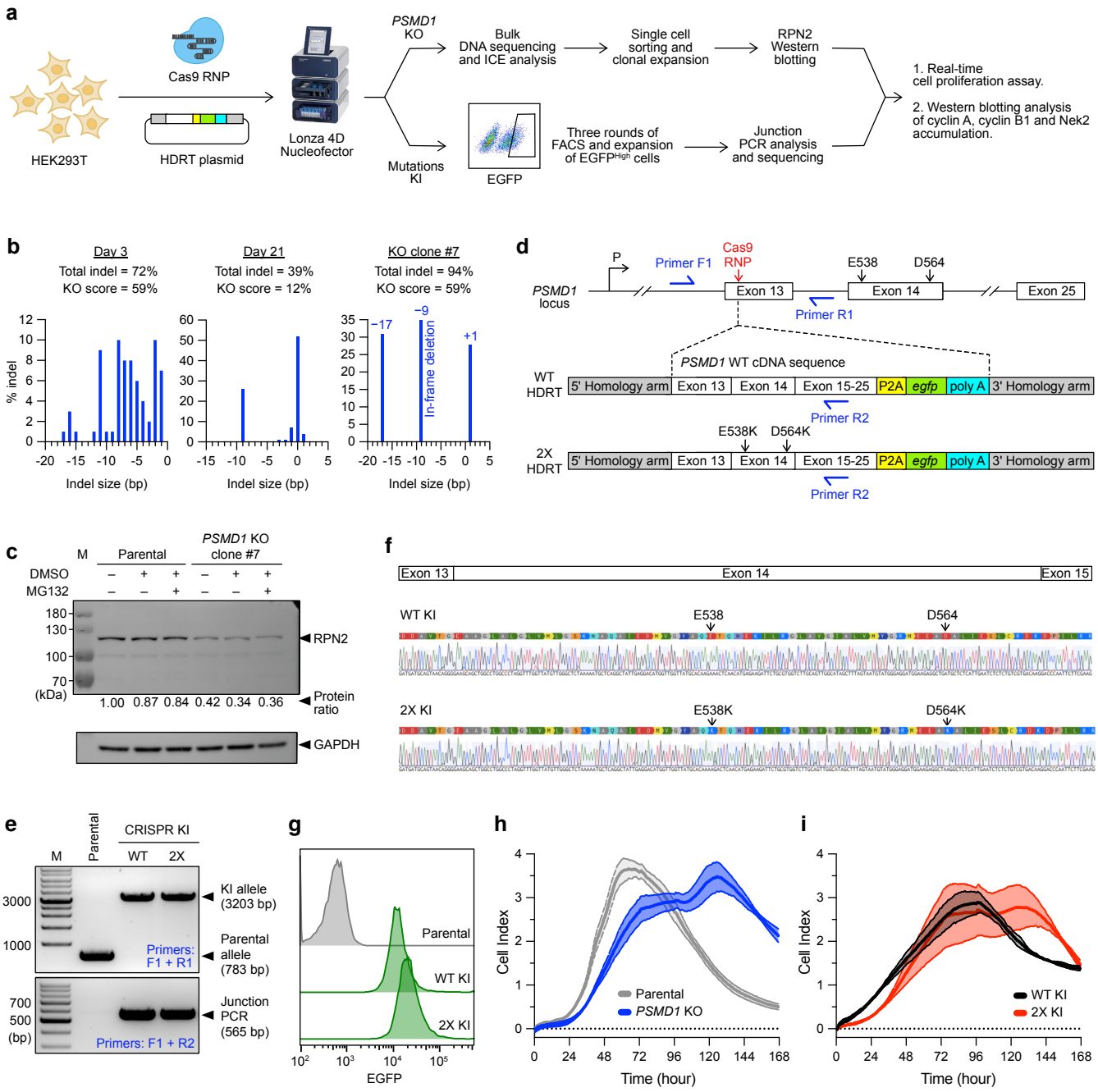

Supplementary Fig. 16. CRISPR gene editing of PSMD1 (RPN2). *Experimental workflow of PSMD1 knockout (KO) and mutation knock-in (KI). Cas9 ribonucleoproteins (RNP) were electroporated into HEK293T cells to disrupt the PSMD1 gene. Edited cells were analyzed by DNA sequencing, single-cell sorted for clonal expansion and confirmed by Western blotting. For KI experiments, plasmid DNA encoding the homology-directed repair templates (HDRT) was co-electroporated with Cas9 RNPs to introduce targeted mutations into the endogenous PSMD1 locus. Mutant cells were enriched using an EGFP reporter strategy and confirmed by genomic PCR and DNA sequencing.* ***b****, Sanger sequencing and ICE analysis of the PSMD1 KO cell population on day 3 and 21 post editing and the isolated KO clone #7. Bar graphs show the percentages of insertion or deletion (% indel) and indel size at the Cas9 target site. Total indels and KO scores were determined by ICE analysis. c, Western blotting analysis of*

RPN2 abundance in the parental HEK293T and PSMD1 KO clone #7 under MG132 or DMSO treatment. GAPDH serves as a loading control. Relative protein ratios were determined by protein band intensity using ImageJ. d, Design of the HDRT, encoding the cDNA sequence of PSMD1 exons 13–25 and an egfp reporter for selection. WT HDRT contains the wild-type cDNA sequence and 2X HDRT the point mutations E538K and D564K. CRISPR-mediated KI enables the insertion of PSMD1 cDNA and a polyA sequence at exon 13, bypassing the endogenous PSMD1 transcription. Primer F1, R1 and R2 (positions indicated) were used for PCR validation. e, Genomic PCR analysis of WT and 2X KI clones. Successful KI yielded a 3,203-bp product, while the endogenous allele generated a 783-bp fragment. Junction PCR using primers F1 and R2 produced a distinct 565-bp amplicon. f, Sanger sequencing of junction PCR products confirmed the targeted insertion at the PSMD1 locus. g, Flow cytometry analysis showing stable EGFP expression in mutant KI clones. h, Cell proliferation analysis of parental HEK293T cells versus PSMD1 KO clone using xCELLigence Real-Time Cell Analysis (RTCA). Cell density was measured by electrical impedance and presented as cell index. i, Cell proliferation analysis of WT versus 2X KI clones using RTCA.

We hypothesized that the 2X mutations will impair the binding of ubiquitinylated substrates to RPN2, thereby compromising proteasome function and cell growth. Supporting this, immunoblotting analysis after MG132 treatment revealed accumulation of cyclin A, cyclin B1 and Nek2 – proteins that haven been reported to be K11/K48 ubiquitinated during cell cycle arrest by Meyer and Rape (PMID: 24813613) – as well as the overall ubiquitin pool. Without MG132 treatment, the differences between 2X KI and WT KI were less pronounced but the trend still held. We tried very hard to obtain K11-linkage-specific ubiquitin antibodies through different venders, but such an antibody cannot be made available in the past four months. Therefore, our assay is limited to ascertain whether the RPN2 mutation (2X KI) resulted in increased K11-linked ubiquitination.

Nonetheless, these genetic and functional studies demonstrated that the conserved residues mutated in RPN2 contributed to recognition and degradation of potentially K11/K48-branched ubiquitinated substrates, and are thus critical for normal cell proliferation and potentially stress resilience. Importantly, our findings were in agreement with the preprint by Haselbach and co-workers (https://doi.org/10.1101/2025.04.07.647569) that reported slightly reduced cell proliferation upon the introduction of Q537K, Q538K, and Q549S mutations to RPN2 and increased accumulation of Securin, which is K11/K48-ubiquitinated through the concerted work of APC/C, UBE2C and UBE2S.

A new **Supplementary Fig. 17** that describes the effects of RPN2 mutations was included as shown below. We hope the reviewer will find these efforts acceptable.

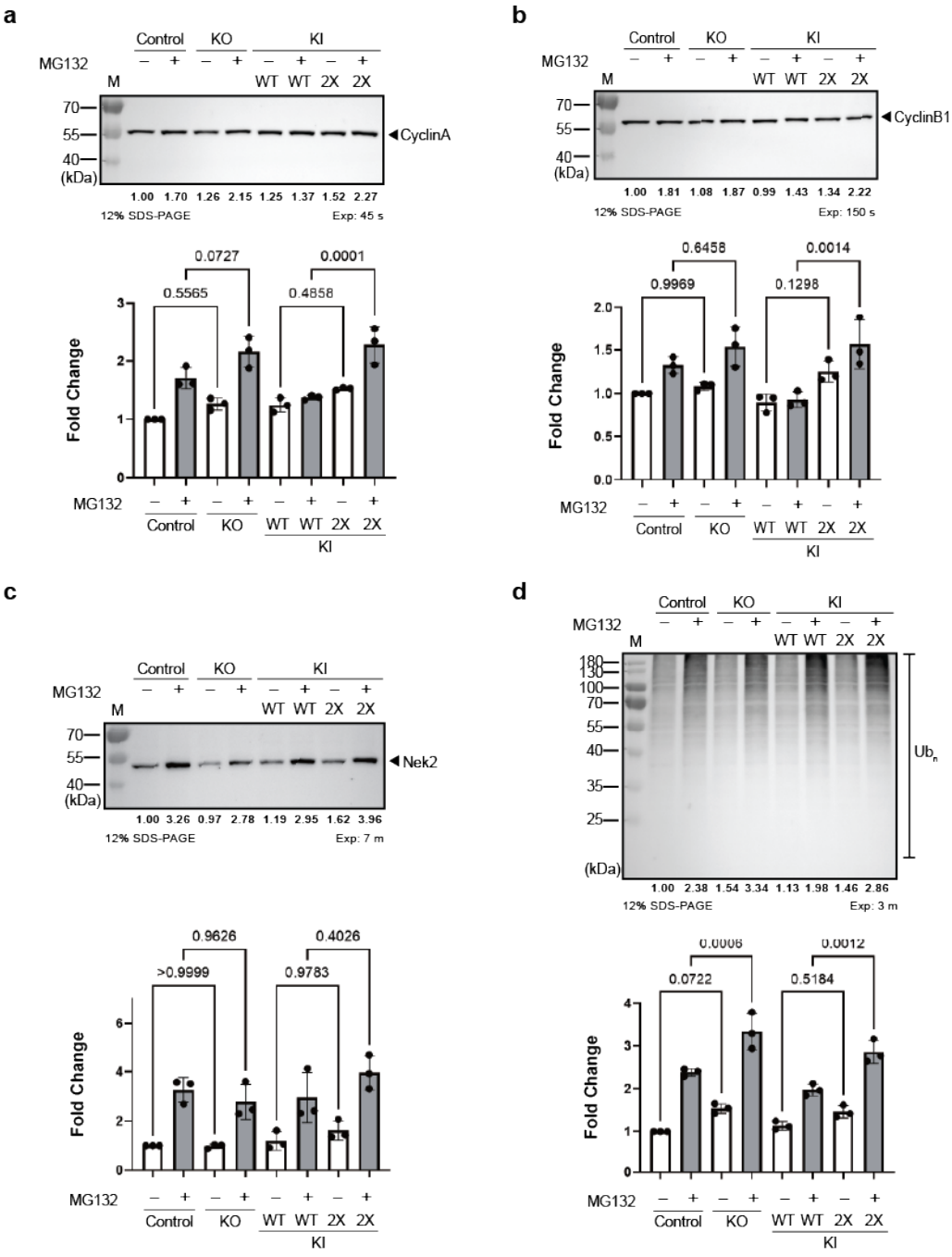

Supplementary Fig. 17. Western blot analyses of the effects of RPN2 mutations. *Representative Western blot results are shown for cyclin A (**a**), cyclin B1 (**b**), Nek2 (**c**) and ubiquitin (**d**) with and without MG132 treatments. All cells are treated with nocodazole for cell cycle arrest. Untreated control, CRISPR/Cas9-edited heterozygous KO, KI with WT and 2X are indicated. Quantitation of band intensities are shown below individual lanes. Further quantitative analyses of technical triplicates are shown below as bar charts with the P-values indicated above the individual pairs.*

7. The dissection of UbI, UbII, UbIII, and UbIV, interactions in the RP is really excellent. The dissertation and figures provided are very clear. Concerning UbIV and the positioning role of UbIII, in line 205: "Given the sparse contacts made by the K11-linked UbIII with RPN2, the primary role of UbIII appeared to restrict the conformational space available to UbIV for positioning it to the new Ub binding groove formed by RPN2 and RPN9." Did authors analyse the position of equivalent UbIV in the complex containing K11-only substrate? How this UbIV and UbIII are accommodated? This is relevant since K11-chains are described in the literature and more abundant than branched forms. Furthermore, when branches are formed, it is expected that K11 linkage to be maintained in the growing branched chain, which is not the case of Sic1PY-Ubn(K63R) generated in this work. Could authors shed light to these issues?

We appreciate the reviewer's comment about the potential binding mode of a long K11-only Ub chain in the equivalent position as the Ub_{IV} reported in our study. Despite extensive image classification of the K11-only Ub chain-containing 26S proteasome, however, we could not detect any additional density at the position corresponding to Ub_{IV} (**Figure R6**), suggesting that the described RPN2 Ub-binding site can distinguish between different linkage types and that the alternating K11-K48 linkage is necessary for the Ub chain to form the more abundant contacts with RPN2 and RPN8 that cannot be achieved by K11-only Ub chains.

David Haselbach and co-worker recently published a preprint in April 2025 (https://doi.org/10.1101/2025.04.07.647569) describing the structural basis of a K11/K48-branched tri-Ub that shows essentially the same binding mode as reported in our current study. In their study, however, they used APC/C. UBE2C and UBE2S to generate K11/K48-branched Ub modified securin, but they did not provide sufficient information in their supplementary data regarding the Ub chain length distribution either by size exclusion chromatography or by SDS-PAGE as they did in greater details for the homotypically K48-linked Ub-GFP-35 in the same preprint. What they presented in their Fig. 2 is the Gauss low-pass filtered cryo-EM map superimposed with a K11/K48-branched tri-Ub chain that binds to the groove between RPN2 and RPN10 as we reported herein. In principle, UBE2S could install multiple K11-linked Ub chains from the branching point similar to our K11-only Ub chain, but they did not report the additional K11-linked Ub EM density beyond the K11-linked Ub from the proximal Ub (equivalent to our Ub_{III}), consistent with our finding reported in **Figure R6** shown below.

We have revised **Supplementary Fig. 13** (formerly **Supplementary Fig. 8**; see below) to improve the clarity and use the same color scheme used throughout the manuscript.

We hope the reviewer will find these revisions satisfying.

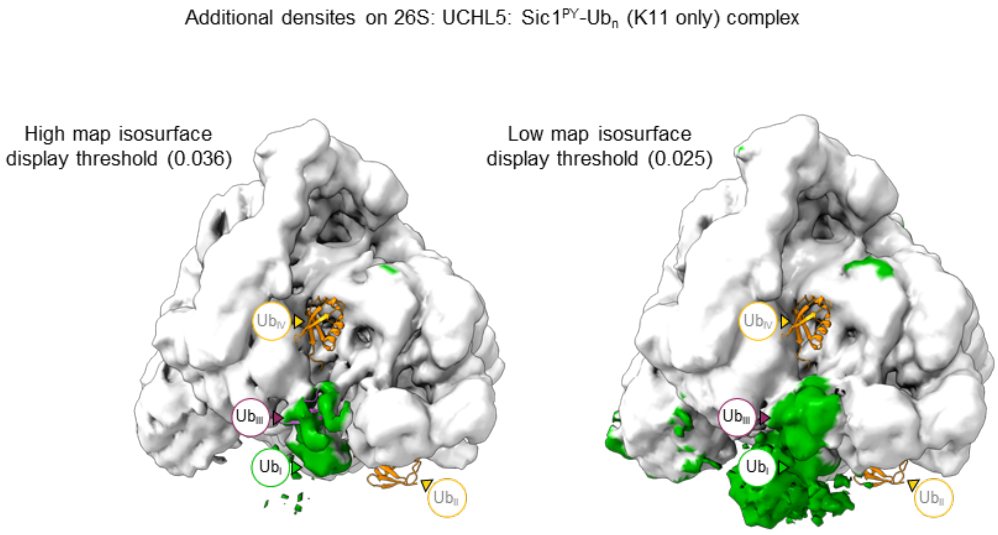

Figure R6. Cryo-EM analysis of the human 26S proteasome supplemented with $Sic1^{PY}$-Ub_n(K11only) (homotypically K11-linked Ub chain). *The cryo-EM map is shown in two different thresholds with the EM density corresponding to the Ub moieties colored in green. The cryo-EM is superimposed with the atomic structures of the K11/K48-branched Ub chain, i.e., $Sic1^{PY}$-Ub_n(K63R). Even at a lower threshold, we did not observe additional density that extends from the K11-linked Ub_{III} towards the position of the K48-linked Ub_{IV}.*

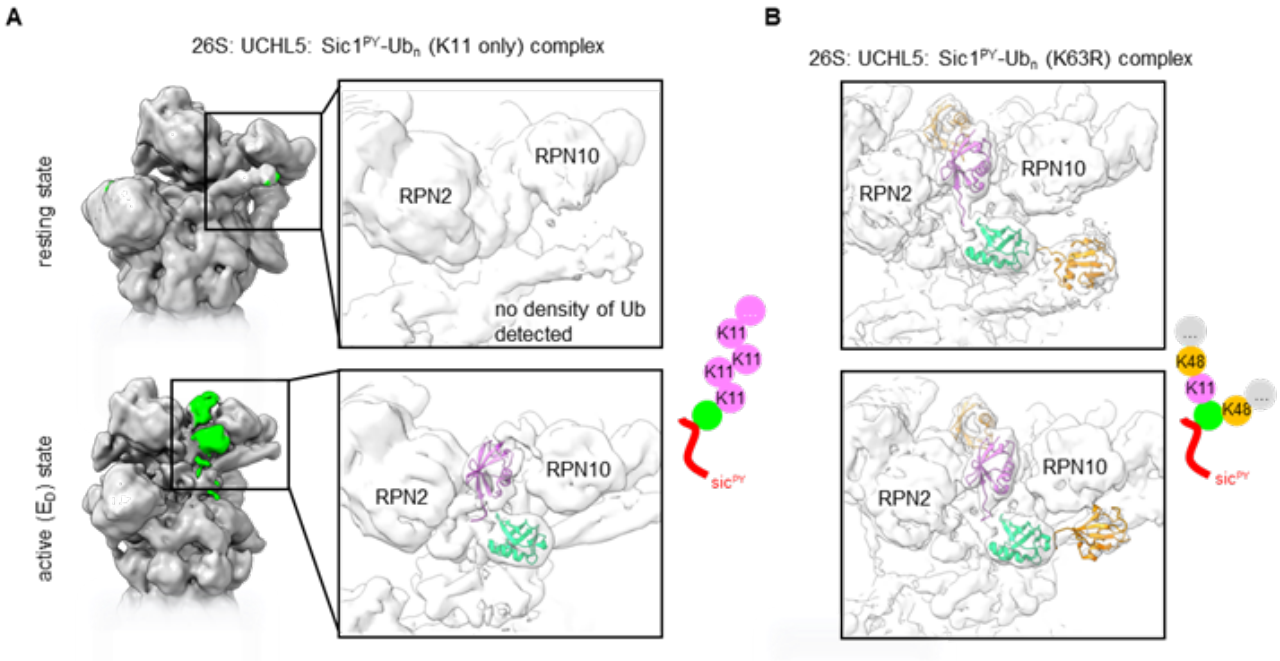

Supplementary Fig. 13. Newly identified K11-linked Ub binding groove is specifically tailored for K11-linked Ub chains. *The comparison of cryo-EM maps of the 26S proteasome in complex with the K11-only ubiquitin chain (a) and the K11/K48-branched ubiquitin chain (b) reveals significant differences. The K11-only ubiquitin chain was observed in the E_D state within the K11-linked ubiquitin binding groove (highlighted in green), but it was absent in the resting (E_A) state. Furthermore, no EM density was detected near the RPT4/5 CC, which binds to the K48-linked ubiquitin extending from the proximal ubiquitin.*

8. In line 226, it is mentioned: "In contrast, in the ED:Ub4 state, the interaction network between the RPN2 and UbIV underwent rearrangements resulting in reduced intermolecular hydrogen bonds and salt bridges (Supplementary Table 1)". However, in the following paragraph and in Supplementary Table 1 no decrease of salt bridges between UbIV and Rpn2 is shown. Moreover, the overall decrease of contacts is very mild. Could authors fix and argue this inconsistency?

We thank the reviewer's suggestion to improve our statements. According to the ePISA (https://www.ebi.ac.uk/pdbe/pisa/) analysis of the interactions involving Ub_{IV} in the E_B:Ub_4 and E_D:Ub_4 states, there are some differences in the intermolecular interactions between the two states, as shown in the **Supplementary Table 6** (formerly **Supplementary Table 1**). We agree with the reviewer that the overall change in the contacts and the change in the interaction area (**Supplementary Table 6**) is marginal. We therefore revised the statement as follows accordingly (page 7, first paragraph):

"In the E_D:Ub_4 state, the interaction network between the RPN2 and Ub_{IV} underwent some rearrangement (Supplementary Tables 6-7)."

We hope the reviewer will find the revision acceptable.

Additional points:

1-Fig. 3 legend shows errors in panel labeling. "b" and "c" are swapped.

Corrected

2-line 140, "Fig. 1e" should be "Fig. 1f"
Corrected

3-line 173, "Fig.1d-f" should be "Fig. 1e-g"
Corrected

4-line 268, "RPT11" should be "RPN11"

Corrected

5-line 273, "PR" should be "RP"
Corrected

6-line 305, "Walkers" should be corrected. "Walters" is the right name.

Corrected

7-line 329, "Additional contacts made by RPN8, RPN9, and RPN10 may be necessary to generate sufficient multivalency (Fig. 2, Fig. 3a, and Supplementary Fig. 9 and 10)." I don't understand why these figures are cited here.

Only Fig. 2 should be cited here. The cross-referencing has been corrected.
The excess cross-references of these figures are removed.

8-line 338: “The plasmids pRSFduet_His-TEV-gsggs-Ub(WT), pRSFduet_His-TEV-gsggs-Ub(K0), pET21d_His-hE1, pETduet_His-SUMO-gg-UBCH7, pGEX_TEV-SENP2, pMBP_TEV-Rsp5-WW3-HECT, and pMBP_TEV-Rsp5 WW3-HECT_GML were synthesized by (GeneScript, USA).”
This sentence is not clear and it seems to be incomplete : what was synthesised by who?

The mentioned plasmids were synthesized by GenScript, USA. The sentence has been corrected to clarify this.

9-line 358: wrong heading

Corrected

7-line 796, "fffinity" should be fixed
Corrected

8 -line 314, in the paragraph: "The conformational changes within the ATPase assembly were reminiscent of the previously reported activation mechanism of archaeal PAN ATPase52, and the activation mechanism of the ATPase unfoldase activity upon Ub binding to the proteasomal Ub receptors53." In this context it would be good to reference Ding et al., 2019 (10.1016/j.molcel.2019.01.018) since it is a relevant work on the effect of tetraubiquitin on proteasome conformations.

We appreciate the reviewer’s correction, which has been included in the revision.

9-in Supplementary Information (page 1), "Supplementary text" is mentioned in the index, but missing in the document. If there's a whole "Supplementary text" missing, it needs to be revised.

There is no Supplementary text with this submission. We removed this item from the Supplementary Information.

10- Supplementary. Fig. 12 legend shows errors in panel labeling. "e" doesn't exist, it should be "d". "d" should be "c". "b" and "c" should be corrected.

In general, the good correspondence of figures, panels in the text should be doublechecked.

We thank the reviewer for the careful proofreading. All the typos and inaccuracies pointed out by the reviewer have been corrected.

Reviewer #2 (Remarks to the Author):

The authors reconstituted a functional 26S proteasome complex containing a specially engineered K11/K48-branched polyubiquitinated substrate and determined multiple cryo-EM structures that reveal how the proteasome recognises such branched ubiquitin chains. Notably, they identified a previously uncharacterised, multi-subunit "groove" on the 19S regulatory particle—formed by RPN2, RPN8, RPN9, RPN10, and RPN11—that selectively accommodates the K11-linked branch, thus enhancing substrate affinity and driving the proteasome's catalytic cycle.

The manuscript is logically structured and clearly written overall. The key findings are adequately supported by the presented data. However, the authors attempted to visualise the substrate and UCHL5 in the cryo-EM density maps, no density was apparent—likely due to the proteasome's intrinsic dynamics. To further probe these interactions, crosslinking mass spectrometry (MS) was employed, but concerns about the design and execution of the crosslinking experiments limit the reliability of those particular findings.

Meanwhile, the crosslinking MS community has established robust and continually evolving protocols for public data deposition. Following the reporting standards outlined in "Toward Increased Reliability, Transparency, and Accessibility in Cross-linking Mass Spectrometry" (PMID: 33065067), I strongly encourage the authors to deposit the crosslinking MS datasets in PRIDE/ProteomeXchange to ensure transparency and reproducibility.

To address reviewer comment, we deposit raw files as well as tables containing all identified unique crosslinked peptides, crosslinked peptide spectra matches and proteins for crosslinking experiments to Pride/ProteomeXchange under the accession number PXD064931 (sample prepared without substrate) and PXD064932 (sample prepared with the $Sic1^{PY}$-Ub_n substrate).

As data were acquired using MS2-MS method (recommended in PMID: 33065067), mzIdenML1.2.0 format cannot be used.

Comments and concerns:

The groove surrounded by RPN2, RPN11, and RPN10 has recently been reported as a binding site for the PITH domain as well. (bioRxiv https://doi.org/10.1101/2024.11.08.622741, https://doi.org/10.1101/2024.12.04.626795, https://doi.org/10.1101/2024.11.08.622731) Could you discuss it and support the biological impact of your finding?

We thank the reviewer for pointing out this preprint that shows the overlapping binding mode of PITH domain (PITHD1) to the pocket formed by RPN2, RPN10 and RPN11. In the Fig. 2E of their preprint, the authors showed that RPN2 uses E358, which is one of the two conserved residues among RPN1 and RPN2 homologs as we illustrated in our Figure 3, to form bipartite hydrogen bonds with PITHD1, suggesting the overlapping function of being targeted by PITHD1 in their study and the K48-linkage between Ub_{III} and Ub_{IV} in our study.

Note that the same group published a preprint (https://doi.org/10.1101/2025.04.07.647569) describing the structural basis of a K11/K48-branched tri-Ub that shows essentially the same binding mode as reported in our current study. In their preprint, it is stated that “Notably, the

trajectory of the K11 branch overlaps with the binding site of PITHD1, a protein we identified as a proteasome inhibitor (ref. 18 in the manuscript). This spatial overlap suggests a mechanism where PITHD1 specifically interferes with the recognition of K11/K48 branched chains, potentially functioning as a mitosis-specific proteasome inhibitor."

They further used an inducible-Cas9 platform to demonstrate the functional contributions of RPN2 and RPN10 in proteasome-mediated clearance of securing, which is potentially K11/K48-linked in their genetic analysis and targeted by the same multi-subunit pocket on the 19S RP as we reported in this study. We have included discussion about their findings in the penultimate paragraph of the Discussion as follows:

"*Recently, Haselbach and colleagues reported the cryo-EM structure of a K11/K48-branched tri-Ub that shows essentially the same binding mode as reported in our current study.*[67] *Mutations in RPN2 and RPN11 result in accumulation of securin, a model substrate used in their study to be K11/K48-ubiquitinated through the concerted work of APC/C, UBE2C and UBE2S. Meanwhile, Haselbach and colleagues also reported in a separate study the cryo-EM structure of the 26S proteasome in complex with PITHD1 that functions as an proteasome inhibitor in the context of cellular dormancy.*[68] *PITHD1 inhibits the proteasome in a triple lock mechanism by targeting the same K11-Ub chain binding groove as we reported herein through a folded PITH domain and the insertion of an extended tail into the ATPase gate that prevent substrate entrance into the 20S CP. The overlapping binding mode between the PITH domain and the K11-linked Ub chain may suggest the interference of the recognition of K11/K48-branched Ub chains by PITHD1 as a mechanism to inhibit the proteasome during mitosis*."

We hope the reviewer will find the addition satisfactory.

(Line 689)
The authors indicate that the functional 26S proteasome complex used for XL-MS was prepared "in the same way as for the cryo-EM experiment." However, ATP—containing a primary amine—can quench NHS-ester crosslinkers, and β-mercaptoethanol (βME) further disrupts crosslinking reactions. Consequently, these conditions likely explain why crosslinks between the proteins of interest were barely detectable, and why almost no crosslinks were observed among the proteasome subunits.

This concern is valid; however, the presence of ATP is essential for the proper function and assembly of the 26S proteasome. Therefore, we decided to include ATP in the sample. We found that the addition of ATP did not cause significant issues in our XL-MS experiments. In fact, we were able to identify more than 300 unique crosslinked (XL) peptides, including 200 inter-chain XLs between 31 proteins (**Supplementary Table 3-4**). This indicates that despite the presence of potentially quenching additives, we successfully crosslinked the 26S proteasome subunits, with an interaction network that aligns with the known structure of the complex. We assume this is because at least part of the ATP is trapped inside the ATP-binding sites in the 26S AAA+ subcomplex, limiting their reactivity with the crosslinker.

Why did the authors use only 0.08mM DSSO?

The concentration of DSSO was set to 0.08 mM based on the molar ratios between the 26S proteasome complex and the crosslinker, equating to a 300-fold excess of crosslinker,

following previous publications (PMID: 28821611; PMID: 3072309). We have included a reference and description in the Materials and Methods section (page 18) as follows:

"The formed complex samples, with and without the substrate, each containing 50 µg of the human 26S proteasome (UBPBio, USA) in a total volume of 100 µL were then individually cross-linked using disuccinimidyl sulfoxide (DSSO) at a final concentration of 80 µM for 1 hour following previously described protocols[82]. The amount of DSSO equates to a 300-fold excess of crosslinker to the 26S proteasome."

Have you verified the effectiveness of the DSSO crosslinking reaction by running an SDS-PAGE gel or Western blot post-crosslinking? It would be helpful to include the corresponding Coomassie-stained gel or Western blot figure in the supplement.

We appreciate the reviewer for the suggestion. While determining the optimal amount of crosslinker via SDS-PAGE is a common method, analyzing the 26S proteasome complex—a 2.5 MDa protein complex—by SDS-PAGE or Western blot post-crosslinking presents significant challenges. To address these concerns, we have included supplemental tables listing all identified crosslinkers.

I also recommend performing a titration of the DSSO crosslinker to confirm optimal crosslinking conditions. Even if the crosslinking is carried out successfully, offline peptide fractionation is strongly advised before LC-MS analysis. This step helps remove shorter (or less-charged) linear peptides, thereby enhancing the identification and detection of crosslinked peptides.

While offline fractionation does increase the number of crosslinkers, the relative simplicity of the 26S proteasome complex and the limited sample amount (50 µg for crosslinking analysis) led us to employ a gas-phase separation strategy. We used high-field asymmetric waveform ion mobility spectrometry (FAIMS) (PMID: 32643919) and collected MS data using 5 CV settings for FAIMS.

(Line 711)
The authors report that MS1 and MS2 scans were acquired in the Orbitrap at resolutions of 60,000 and 30,000, respectively, while MS3 scans were acquired in the ion trap. Could you clarify why lower resolutions were chosen in these experiments?

In this study, we used the standard MS2-MS3 method for MS cleavable crosslinkers such as DSSO (PMID: 28524877; PMID: 27626298)

MS3 is performed in an ion trap to improve the duty cycle. MS3 scans run in parallel with high-resolution MS2 scans, increasing identified crosslinkers. Crosslinked peptides can be identified from high-resolution MS2 scans and MS3 scans using a mass difference of 31.9721 (PMID: 28524877).

I suggest that the authors move to more simple MS2 methods - they give a more reliable FDR, and they are easier for a simple sample like a single complex.
https://www.nature.com/articles/s41467-022-31701-w

We appreciate the reviewer's suggestion. Based on previously published 26S proteosome studies, we selected the MS^2-MS^3 method. We also re-analyzed all XL-MS data using the newly updated Proteome Discoverer 3.2 XlinkX 3.2, which has improved FDR calculations for unique crosslinkers as well as CSMs. We felt that the updated analyses provided sufficient information for such a complex system. We hope the reviewer will agree with our assessments and updates.

(Supplementary Fig. 6.)
It is currently very difficult to draw concrete conclusions about the interaction network derived from the XL-MS analysis. I recommend addressing the following points:
1. Residue Pairs: Could you please provide the specific residue pairs for key crosslinks shown in the network? Additionally, the corresponding MS spectra for the key crosslinks should be included to support your conclusions.

The reviewer's recommendations have been considered. To address this issue, new **Supplemental Tables 3 & 4** have been added to illustrate the identified residue pairs and their interactions between $Sic1^{PY}$-Ub_n, Ub-UCHL5, Ub-RPN13, and UCHL5-RPN8. **Supplementary Fig. 6** has also been updated using xiNET, as shown in a new **Supplementary Fig. 9** (see below), along with structural mapping of the observed XLs using XMAS (shown in **Supplementary Fig. 10 & 11**).

2. Origin of Ubiquitin: Where does the ubiquitin (Ub) depicted in Supplementary Fig. 6(a) originate?
3. RPN1–Ub Crosslinks: Can you explain why no crosslinking was observed between RPN1 and Ub?

We detected one interaction between Ub and PRN1 (Q13200) in the presence of the $Sic1^{PY}$-Ub_n substrate. This corresponds to the cross-link (XL) between RPN1 K747 and Ub (K63R) K6. **Supplementary Tables 3 & 4** have been included in the revised manuscript to list all observed XLs.

Additionally, we have revised **Supplementary Fig. 9** (formerly **Supplementary Fig. 6**) to illustrate all observed XLs using xiNET (https://crosslinkviewer.org/). The revised **Supplementary Fig. 9** depicts extensive XLs between most proteasomal subunits, including alpha (PSA) and beta (PSB) subunits of the core particles. In the compressed ZIP files of **Supplementary Tables 3 & 4**, we have included the FASTA input files necessary for visualization by xiNET. We hope these additions will help the readers to appreciate our XL-MS analyses better.

Without recombinant RPN13-UCHL5(C88A) and $Sic1^{PY}$-Ub_n(K63R), the XLs were more evenly distributed among different subunits. Some XLs were observed for endogenous Ub, UCHL5, and RPN13. When supplemented with an excess amount of recombinant UCHL5(C88A)/RPN13 and $Sic1^{PY}$-Ub_n(K63R), the XLs predominantly enriched between Ub(K63R) and UCHL5, as well as between Ub(K63R) and RPN13, which was expected. Moreover, Ub(K63) was found to cross-link with RPN1, RPN3, RPN7, RPN10, and RPN12.

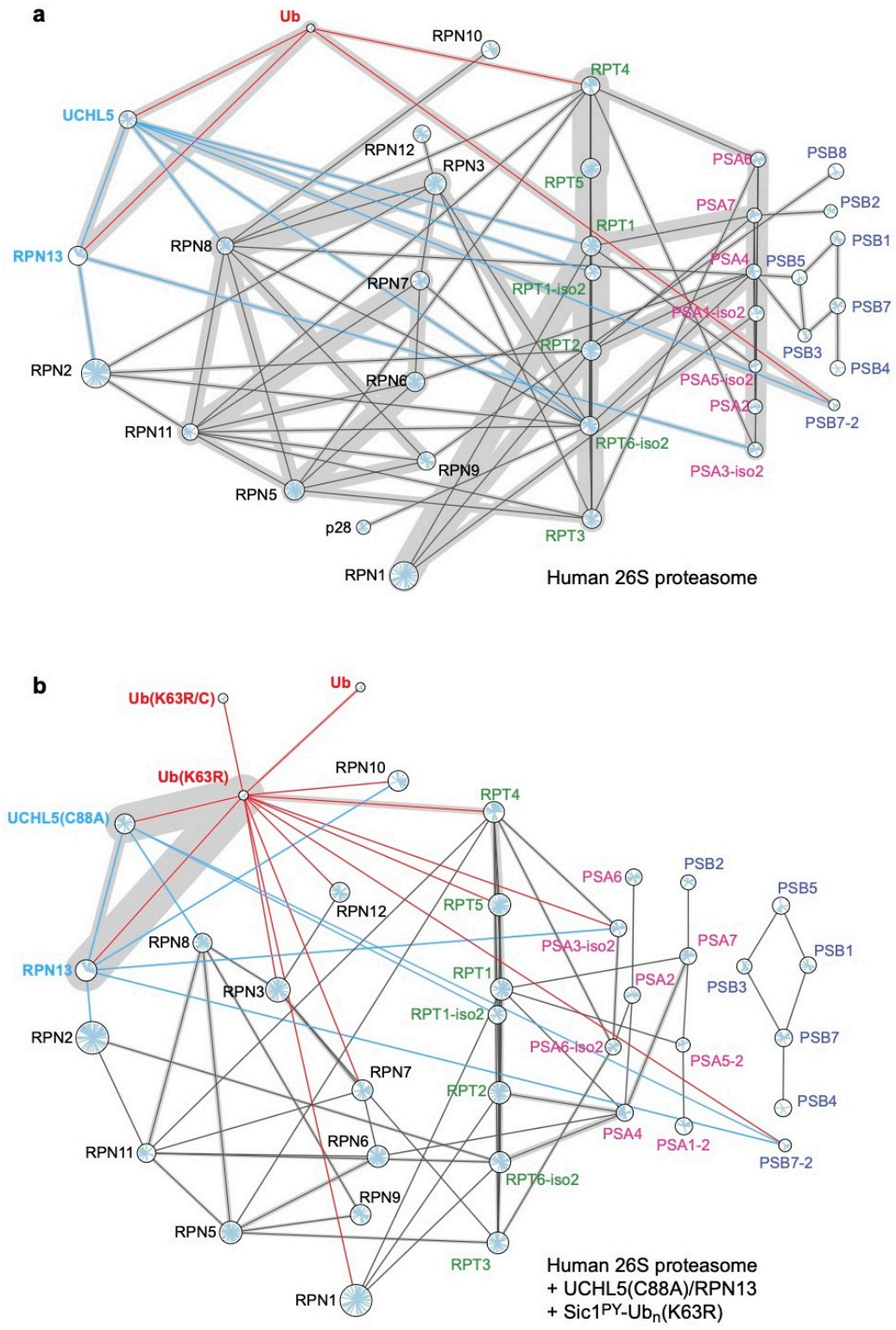

Supplementary Fig. 9. Graphical representation of XL-MS network of 26S proteasome. *The XL-MS data depict the XL network in the human 26S proteasome without (**a**) and with (**b**) the addition of preformed UCHL5(C88A)/RPN13 complex with Sic1^{PY}-Ub$_n$(K63R) spiked with 10% cysteine mutant*

Ub(K63R) for fluorescent labeling. XLs associated with Ub variants are red, those with UCHL5 and RPN13 variants are blue. Thickness of XLs corresponds to the nu*mber observed in datasets. Generated by xiNET (https://cross*linkviewer.org/) *with color modifications for subunit labels and XL types.*

4. Validation with Known Structures: Have you verified that the identified crosslinks (e.g., UCHL5–RPN13, UCHL5–Ub) align with known structural information?

To address the reviewer's comment, we used XMAS as a ChimeraX plug-in (https://doi.org/10.1101/2022.04.21.489026) to map the observed XLs onto the cryo-EM structures, shown in the new **Supplementary Fig. 10**. XMAS revealed that most XLs (92-87%) had Cα-Cα distances within 35 Å when XLs with Ub were excluded **(Supplementary Fig. 10a**). Longer XL distances corresponded to Ubs and are likely artifacts due to XMAS's inability to distinguish different XL peptides from Ubs of the same sequence **(Supplementary Fig. 10c**,**d**). Generally, one Ub in the E_A:Ub_3, E_B:Ub_4, and E_D:Ub_4 states linked with proteasomal subunits within reasonable distances. The inter-chain XL of RPT1 K402-RPN1 K343 and intra-chain XL of RPN3 K461-K503 exceeded 50 Å only in E_A:Ub_3 and E_B:Ub_4 states, reflecting conformational features unique to these states.

For XLs of UCHL5-RPN13 and UCHL5-Ub, we used reported UCHL5 crystal structures in complex with Ub and RPN13 DEUBAD (PDB entries: 4UEL (PMID: 25702870) and 4wlr (PMID: 25702872)) to map the XLs, all within 35 Å; endogenous Ub showed limited XLs with UCHL5 but not with RPN13 (**Supplementary Fig. 11**).

Overall, our XL-MS data aligns with simpler system crystal structures despite many conformational changes in the 26S proteasomal complex. We included these results in the new **Supplementary Fig. 10**. An additional paragraph was added to the revised manuscript as follows (page 5, first paragraph):

"*Structural mapping of the observed XLs onto the cryo-EM structures of the four different states was carried out using XMAS[56] (Supplementary Fig. 10). The results showed multiple interactions between Ub and several proteasomal subunits and the long XLs (Cα-Cα distances exceeding 35 Å) were generally associated the Ubs. These long XL distances associated with Ubs were likely artifacts, due to the intrinsic difficulty to unambiguously distinguish between XL peptides with identical sequences but from different Ubs (Supplementary Fig. 10c,d). Some XLs associated with the 19S RP subunits were found to be larger than 35 Å only found in the E_A:Ub_3 and E_B:Ub_4 states but not in the E_D:Ub_4 state, reflecting the conformational changes between these functional states (Supplementary Fig. 10a). When the XLs were mapped onto the crystal structures of UCHL5-RPN13-Ub[57,58], all XLs were within 35 Å, indicating the robustness of our XL-MS analysis when applied to a simpler quaternary structure (Supplementary Fig. 11).*"

We hope the reviewer will find the updated structural mapping satisfactory.

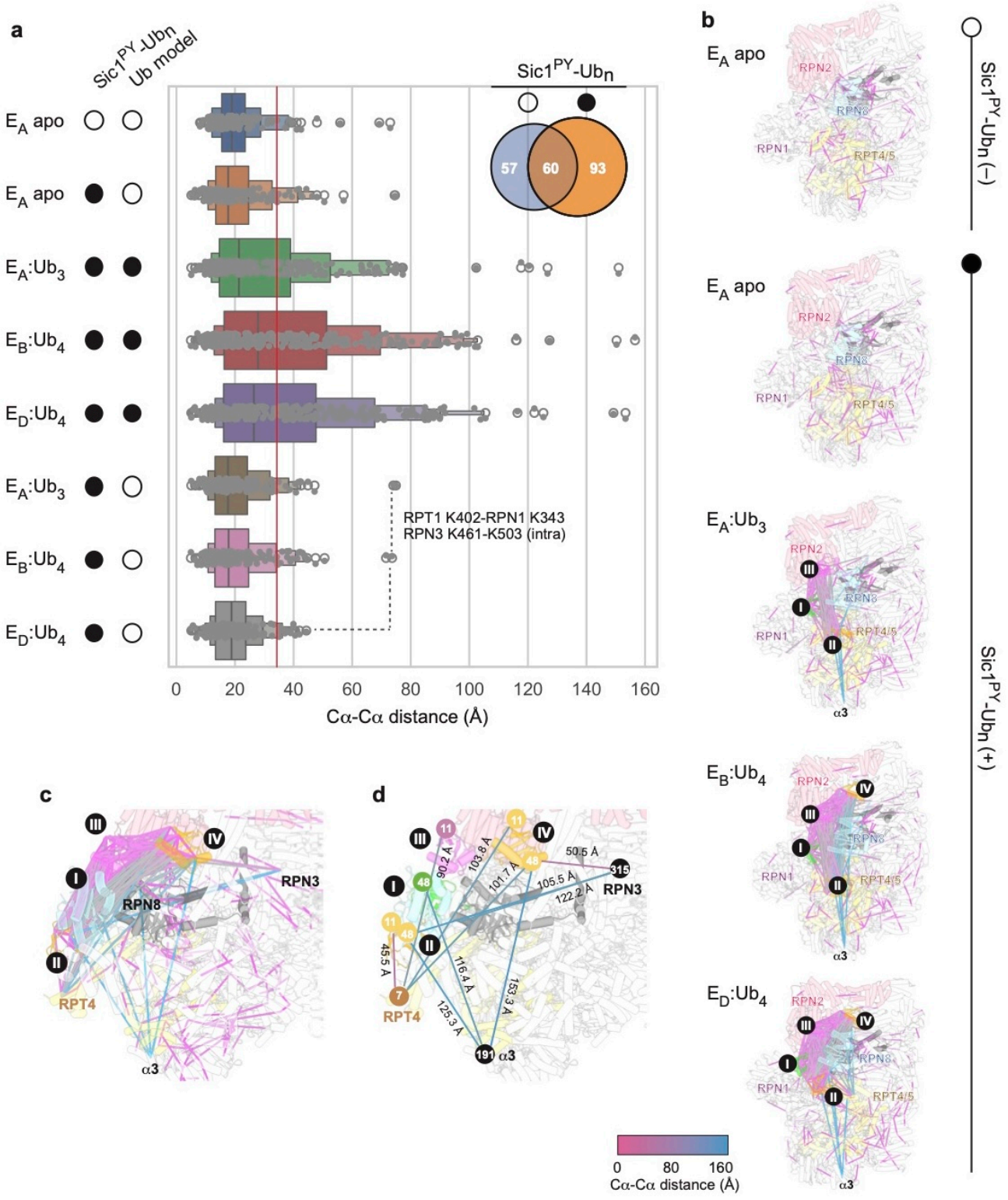

Supplementary Fig. 10. Structural mapping of XL-MS data onto the cryo-EM models of 26S proteasome. *(**a**) Distance distributions of observed XL lysine pairs in different functional states – apo E_A (PDB entry: 8JRI), E_A:Ub_3 (PDB entry: 8JRT), E_B:Ub_4 (PDB entry: 8JTI) and E_D:Ub_4 (PDB entry: 8K0G) – without and with Sic1^{PY}-Ub_n indicated by open and filled circles, respectively, next to their*

*functional states. The XL distances were mapped by XMAS as a plug-in module within ChimeraX. The distances are defined as the Cα-Cα distances between the lysines that are linked by DSSO. To highlight the long distances attributed to XL with Ubs, additional distance distributions were calculated for the E_A:Ub_3, E_B:Ub_4, and E_D:Ub_4 states, excluding the coordinates of the Ubs (bottom three rows), as indicated by open circles in the second column next to their functional state annotations. Two long XL distances beyond 75 Å were observed in the E_A:Ub_3 and E_B:Ub_4 states, corresponding to an inter-chain XL of RPT1 K402-RPN1 K343 and an intra-chain XL of RPN3 K461-K503. These long XL distances were reduced to < 45 Å in the E_D:Ub_4 state, indicating that these XLs captured the conformation corresponding to the E_D:Ub_4 state distinct to the E_A:Ub_3 and E_B:Ub_4 states. Inset: Venn diagram of the overlap of the observed XL between the E_A states without (blue) and with (orange) $Sic1^{PY}$-Ub_n. Only 60 XLs were commonly observed in these two conditions, dominated by the shift of XLs corresponding to the supplemented UCHL5(C88A), RPN13, and Ub(K63R) in addition to $Sic1^{PY}$-Ub_n in the reconstituted 26S proteasome sample. (**b**) Structural mapping of the observed XLs in the apo E_A (±$Sic1^{PY}$-Ub_n), E_A:Ub_3, E_B:Ub_4 and E_D:Ub_4 states rendered by XMAS using ChimeraX. The XL distances are color-ramped from fuchsia to blue, corresponding to 0 to 160 Å, as indicated by the scale bar on the bottom. The subunits of interests and Ub_I-Ub_{IV} are colored following the same scheme in Figure 1e (except RPN1 in white) and in highly transparent cartoon representations. (**c**) Expanded view of the XL mapping of the E_D:Ub_4 state highlighting the long XLs connecting Ubs and RPN3 and α3 subunits. (**d**) Selected XLs that link Ubs to RPN3 and α3 subunits with their distances in Å indicated along the lines connecting the particular lysine residues whose residue numbers are indicated in the filled circles with colors matching the individual Ubs. The XL between RPN3 K315 and Ub_{IV} K48 is 50.5 Å, which is within a reasonable distance range of expected XLs. The long XLs connecting RPN3 K315 and K48 of Ub_I and Ub_{II} beyond 100 Å are likely artifacts due to XMAS's inability to distinguish between different XL peptides arising from different Ubs of the same sequence.*

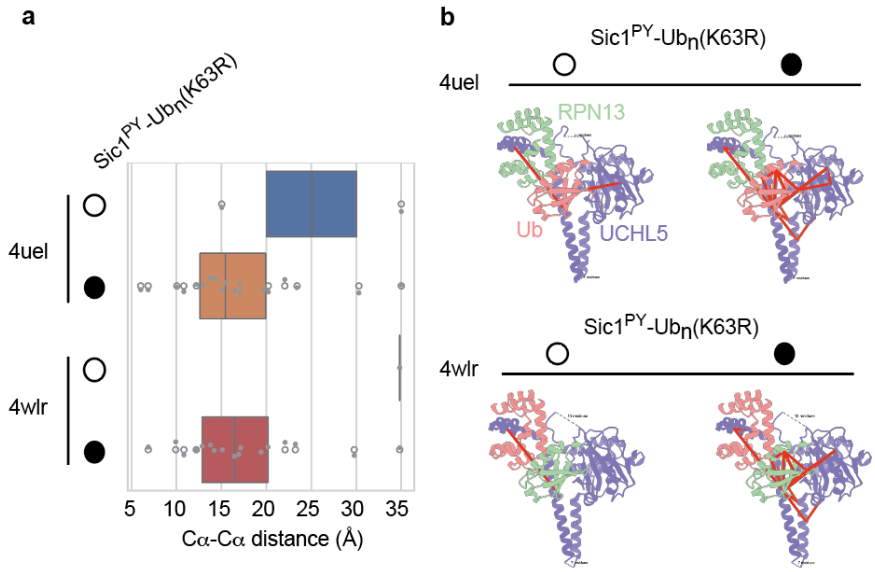

Supplementary Fig. 11. Structural mapping of XL-MS data onto the crystal structures of UCHL5-RPN13-Ub. *(**a**) Distance distributions of observed XL lysine pairs in the two reported crystal structures of UCHL5-RPN13-Ub (PDB entries: 4UEL and 4WLR) without and with $Sic1^{PY}$-Ub_n indicated by open and filled circles, respectively. The XL distances were mapped by XMAS within ChimeraX. (**b**) Structural mapping of the observed XLs on the quaternary structures of UCHL5-RPN13-Ub. UCHL5, RPN13 (DEUBAD) and Ub are colored purple, green and salmon, respectively. The observed XLs are shown in solid red lines.*

5. RPN3–Ub Interaction: RPN3 is unlikely to interact with Ub. Do you have any hypothesis or explanation for this unexpected result? Addressing these questions and clarifying the data would help strengthen the conclusions drawn from Supplementary Fig. 6.

We refer the reviewer to **Supplementary Fig. 10** above, which illustrate the XL mapping of the E_D:Ub_4 state with highlighted long XLs connecting Ubs and RPN3. Specifically, the XL between RPN3 K315 and Ub_{IV} K48 is 50.5 Å, while in the E_B:Ub_4 state, it measures 51.6 Å. Given the heterogeneous chain length of our $Sic1^{PY}$-Ub_n substrate (**Figure 1b**), additional Ubs may extend from Ub_{IV}, bringing it closer to RPN3 and forming the XL. Indeed, we have commented the possibility of another Ub extending from Ub_{IV} in **Supplementary Fig. 20**, which analyzed the possible extension of a K48-linked Ub from Ub_{IV} using previously reported K48-linked di-Ub structures. In this case, the PDB entry 2KDF could fit into the pocket between RPN2, RPN9 and RPN8 although we did not observe defined EM density in our structures. Nonetheless, we cannot exclude the possibility of having additional Ub moieties from Ub_{IV}, which could explain why the XL between RPN3-Ub was observed. We hope these updates are satisfactory.

Minor:

(Line 305) "Walkers" needs to be changed to "Walters".

We thank the reviewer for the careful proofreading. This typo has been corrected.

Reviewer #3 (Remarks to the Author):

This paper describes a single particle cryo-EM based investigation into the mode of binding of a K11/K48-branched tetra ubiquitin chain to the human 26S proteasome. Understanding the structural basis of branched ubiquitin chain recognition by the proteasome is an important matter both with respect to the biology of the system and its potential in drug development.

The major problem with the paper as currently presented is the limited resolution of the analysis, particularly in the part of the structure that is most important for this study – the tetraubiquitin chain and its immediate environment. The authors claim to identify each of the ubiquitin molecules as well as the linkage in their cryo-EM map. Ubiquitin chains are assembled by linking the extended single stranded C-terminal tail of one ubiquitin to an amino group (in this case that on the side chain of lysine 11 or lysine 48) on the subsequent ubiquitin molecule. The authors state "Importantly, we unambiguously resolved the cryo-EM densities of a K11/K48-branched tetra-Ub(Ub4) chain bound to the EB and ED states (hereafter EB:Ub4 and ED:Ub4, respectively;)" referring to Figure 1 d-f (here I think they mean Figure 1 e-g) and their supplementary movie.

In my opinion the figure and movie do not unambiguously support their model. Ideally, to do this they should be able to unambiguously trace the complete chains of each ubiquitin and its linkage within their density maps. This does not appear to be the case. In Figure 1 e & f they identify a set of 4 densities which they ascribe to ubiquitin. Although these densities are generally consistent with ubiquitin, the level of detail does not appear sufficient to identify secondary structure detail and hence it is not clear that the ubiquitin molecules have been docked in the correct orientation. For some reason, more detail is shown in Figure 1g. Nevertheless, the densities ascribed to ubiquitin still appear to lack secondary structure detail and the match between the map and fitted models is incomplete with regions of model such as the C-terminal tail of ubiquitin IV falling outside the experimental density and regions of experimental density which are not explained by the model.

In the light of the above comments I recommend that the authors revise their interpretation of the ubiquitin density assignments. It is possible that a detailed consideration of possible docking geometries and agreement with their experimental maps may allow them to identify a unique solution and rule out alternatives. If this could be argued in a convincing and logical fashion I would find the paper acceptable for publication.

We appreciate the reviewer's candid assessment of our modeling quality. To address the reviewer's concerns, we prepared an additional **Supplementary Fig. 6** to illustrate the map-to-structure correlation based on the per-residue Q-scores of individual Ubs. We also presented the map-to-structure correlations for the individual Ubs in unsharpened and sharpened maps (**Figure R7**). The hallmark of the Ub fold, *i.e.*, an α-helix wrapped by a four-stranded β-sheet can be distinguished in these examples. The unique structural feature facilitated the straightforward determination of the Ub orientation and robust rigid body fit of the Ub crystal structures (performed in ChimeraX), followed by molecular dynamics-driven flexible fitting of the atomic coordinates into the cryo-EM map (using *ISOLDE*). Importantly, the per-residue Q-score analyses demonstrated that all Ubs but Ub_{II} exhibited higher Q-scores than the expected values at their respective resolutions. Ub_{II} was significantly less defined in different functional states. However, even in this case, the characteristic Ub fold could be identified.

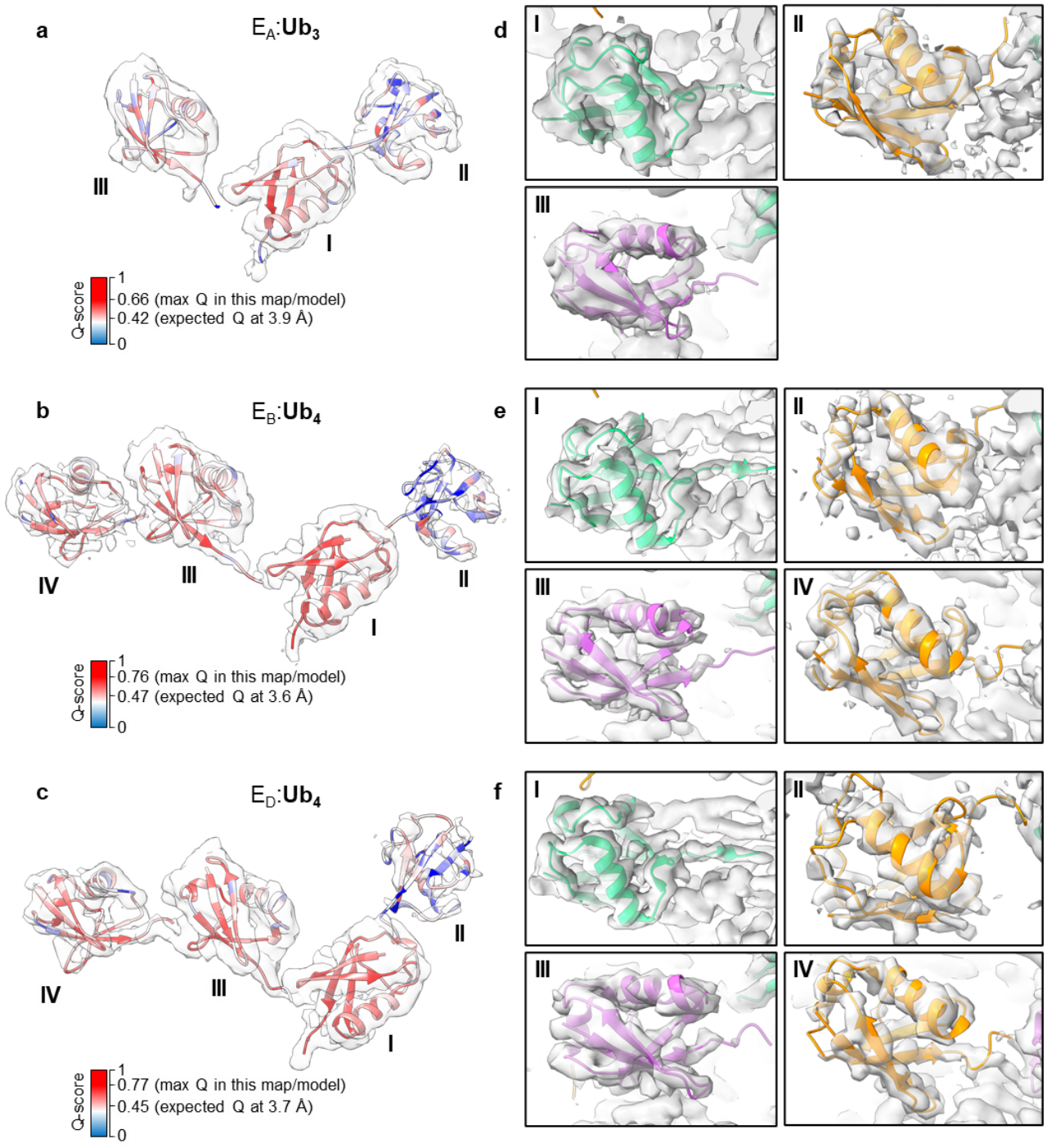

***Supplementary Fig. 6. Structural quality assessments of the K11/K48-branched Ub chain bound to the proteasome**. **a,** The atomic model of the tri-Ub in the E_A:Ub_3 state is shown in a cartoon representation, colored from blue to white to red according to the Q-score, which reports on the quality of the structural model in relation to the corresponding cryo-EM map, shown in a transparent surface. The expected Q-score at the resolution of the cryo-EM map and the maximum Q-score of the tri-Ub model are indicated in the scale bar on the lower left corner. Red and blue colors indicate regions that*

*are better and worse than the expected structural quality at this resolution, respectively. The same Q-score analyses were applied to the tetra-Ub in the E_B:Ub_4 (**b**) and E_D:Ub_4 (**c**) states. In panels **a-c**, the contour levels were set to 5 for all the cryo-EM maps for better comparisons. **d-f,** Superposition of the sharpened cryo-EM maps and the corresponding atomic structures of the individual Ub. The signature thumb-like α-helix of individual Ubs was clearly visible in all the maps.*

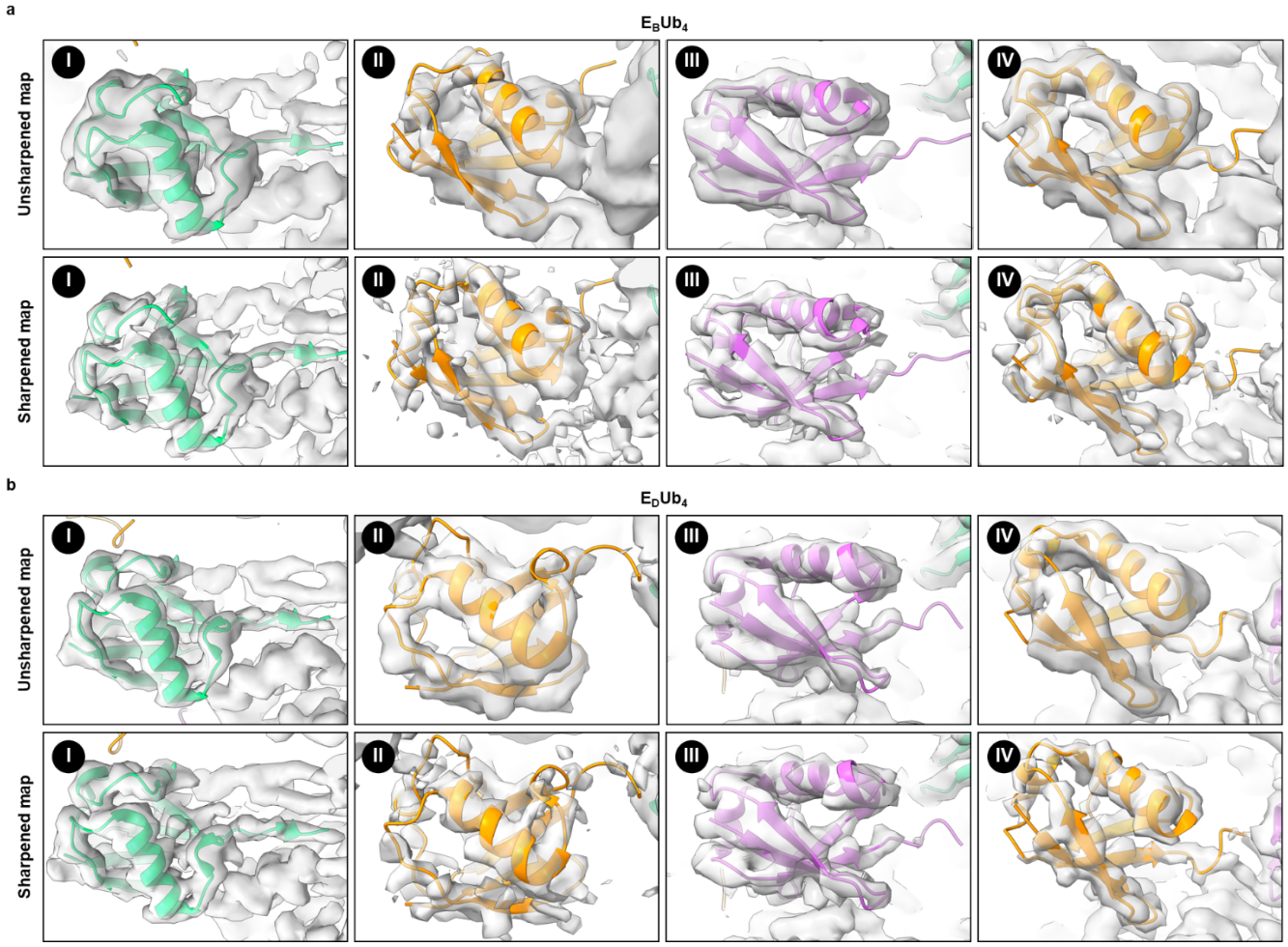

Figure R7. Close-up view of Ub_I to Ub_{IV} densities in unsharpened and sharpened cryo-EM maps of the E_B:Ub_4 and E_D:Ub_4 complexes. *All densities exhibit a clear Ub fold with distinguishable secondary structure elements.*

To further evaluate the robustness of our model-building of the proteasome-bound Ubs, we used DeepMainMast (PMID: 38066344) to automatically trace the Ub backbone based on the cryo-EM density of the proteasome-bound Ub chain, providing only the Ub sequence. Additionally, we used DiffModeler (PMID: 38328203) to model the more dynamic Ub_{II}. As shown in **Figure R8**, the fully automated model building of the tetra-Ub structures in the E_B:Ub_4 and E_D:Ub_4 states are consistent with our manually optimized model. A slight deviation was observed for the Ub_{II} due to the fragmented EM map density, but the resulting structure is consistent with our initial assignment of the K48-linkage.

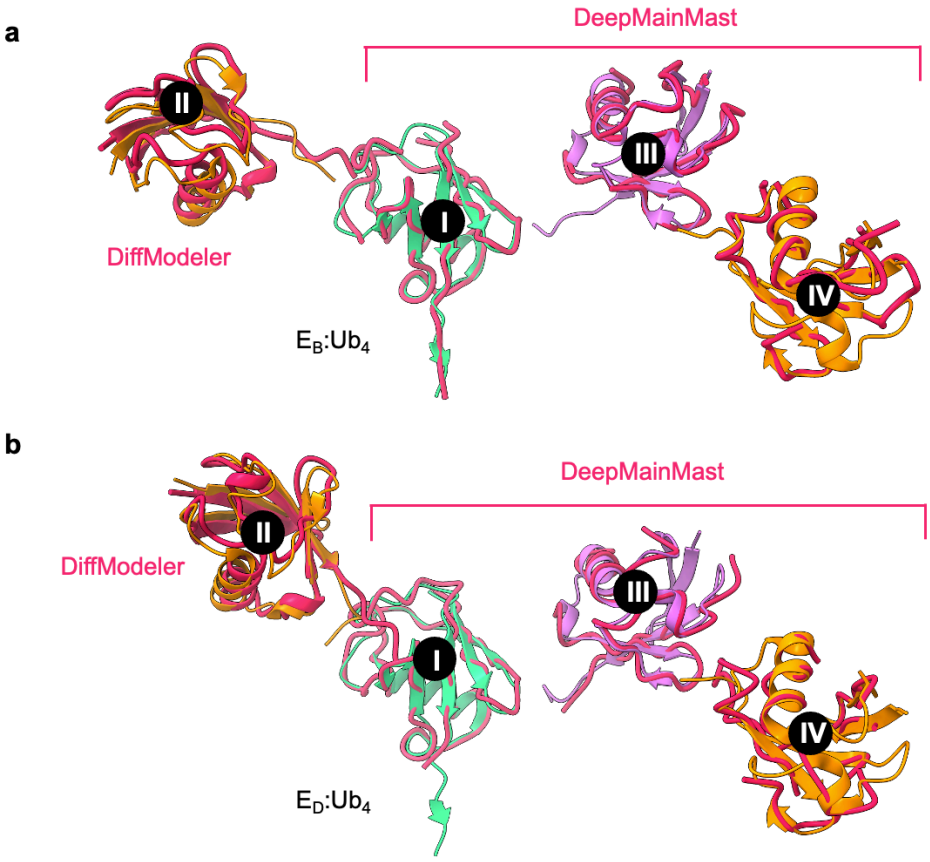

Figure R8. Comparison of the K11/K48-branched Ub chain models generated by machine learning-based automation based on the resolved Ub EM densities. *The structural models of Ub_I, Ub_{III} and Ub_{IV} in the E_B:Ub_4 and E_D:Ub_4 states are built by DeeMainMast shown in hot pink ribbons and superimposed with the manually optimized models in cartoon representations colored in green, purple and orange, respectively. The models of Ub_{II} are built by DiffModeler shown in hot point ribbons and superimposed with the manually built counterparts in orange cartoon representations.*

The robustness of our model-building approach enables confident assignment of linkages within the K11/K48-branched ubiquitin chain and is strongly supported by the experimental cryo-EM density data. Utilizing solution state NMR spectroscopy-restrained molecular dynamics simulations, which comprehensively capture the conformational diversity of ubiquitin across 46 crystal structures (ref. 53 in the manuscript), we evaluated which lysines could credibly form the observed conjugates. This analysis demonstrates that the linkages we report are not only consistent but uniquely plausible, as evidenced by the precise placement and connectivity of Ub densities. Distinct densities were observed connecting the K48 of Ub_I to Ub_{II}, K48 of Ub_{III} to Ub_{IV}, and K11 of Ub_I to Ub_{III}, with no alternative lysines within sufficient proximity to account for these connections. Even the lower Q-scores in the linkage region between Ub_I and Ub_{II}, attributed to the inherently less resolved structure of Ub_{II}, do not undermine the clarity of the linkage at lower map thresholds (new **Supplementary Fig. 7**). These findings, underpinned by high Q-scores and corroborated by map-to-structure correlations, helped us validate the accuracy of our linkage assignments and reflect the reliability of our model-building methodologies.

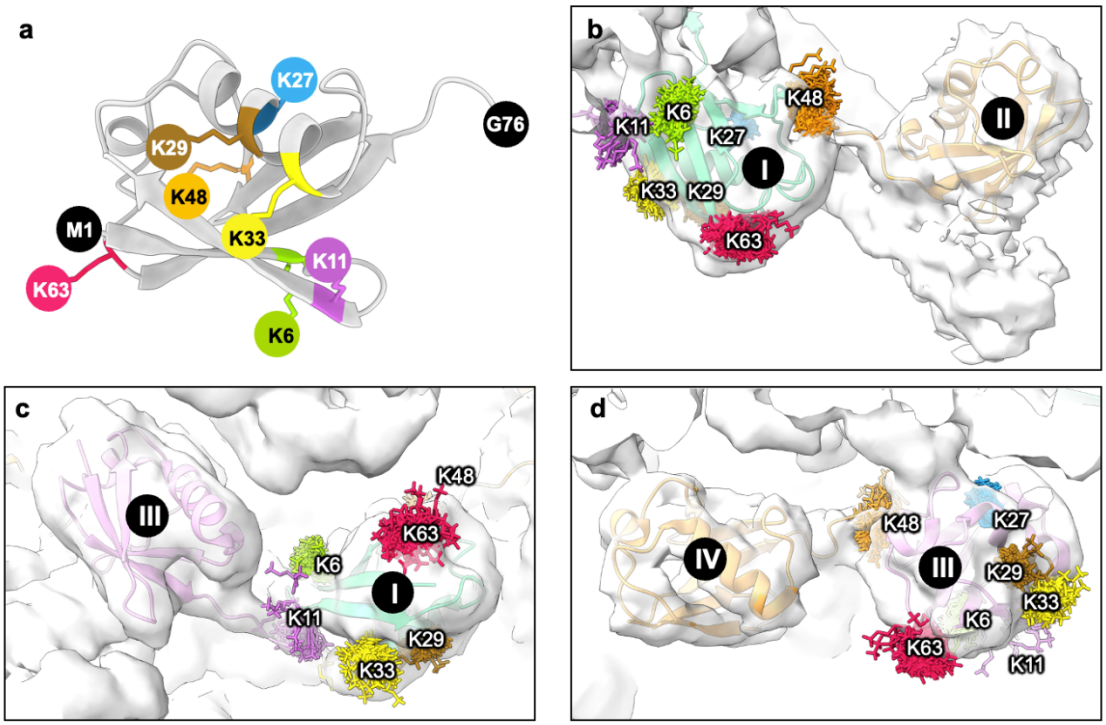

Supplementary Fig. 7. ***Ensemble analysis of potential isopeptide bond linkages of observed Ub EM map.*** *(**a**) Cartoon representation of Ub with the individual lysine positions indicated by different colors. (**b**) Ensemble conformations of the individual lysine side-chains of Ub_I by superpositioning the NMR ensemble structure (PDB entry: 2K39) on the cryo-EM structure of Ub_I with the individual lysine side-chains colored and labeled according to (**a**). The same structural alignment was applied to Ub_I (**c**) and Ub_{III} (**d**). In all cases, the only possible isopeptide linkage corresponds to the one that was reported in this study, which has clear EM density connecting the C-terminus of the other Ub to the isopeptide-linked lysine.*

Regarding the reviewer's comment about "the C-terminal tail of ubiquitin IV falling outside the experimental density and regions of experimental density which are not explained by the model", our response is as follows.

Upon closer examination, the C-terminal tail of Ub_{IV} is indeed aligned with the cryo-EM density, and any appearance of disconnection is solely due to the isosurface display threshold applied in the figures. In **Figure R9** provided below, we have adjusted the threshold to distinctly illustrate the K48-linkage within the EM map for both E_B:Ub_4 and E_D:Ub_4 states. Additionally, the prominent EM density connecting Ub_{III} and Ub_{IV} corresponds to the side-chain of R74 of Ub_{IV}, which forms stable interactions with Ub_{III}. These detailed visualizations confirm the accuracy and robustness of our model-building approach.

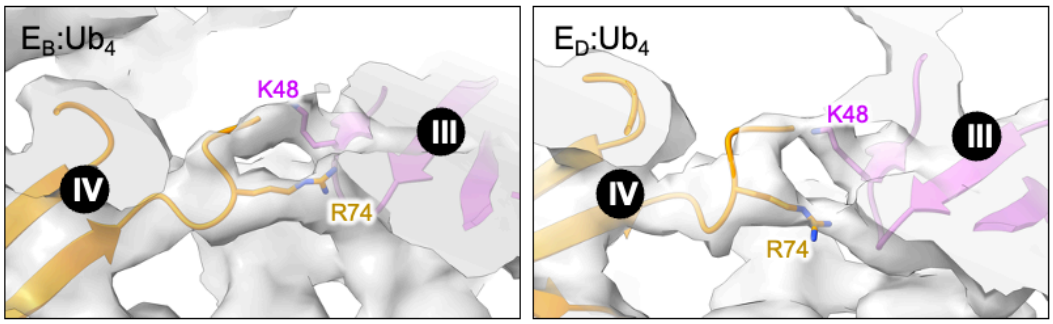

Figure R9. Expanded views of interaction between Ub_{III} and Ub_{IV}. *The thresholds were adjusted to illustrate the K48-linkage within the EM map for both E_B:Ub_4 and E_D:Ub_4 states. Additionally, the prominent EM density connecting Ub_{III} and* Ub_{IV} *corresponds to the side-chain of R74 of* Ub_{IV}*, which forms stable interactions with Ub_{III}.*

With these additional analyses that illustrate the robustness of our cryo-EM model, we have revised our statement in the second paragraph of page 4 as follows:

"*Importantly, we unambiguously resolved the cryo-EM densities of a K11/K48-branched tetra-Ub (Ub_4) chain bound to the E_B and E_D states (hereafter E_B:Ub_4 and E_D:Ub_4, respectively), which showed good per-residue Q-scores[52] for the individual Ubs (Supplementary Fig. 6) and unique spatial distributions of the possible isopeptide bond linkages when considering the conformational landscape accessible to Ub[53] (Supplementary Fig. 7).*"

We hope the reviewer will find these updates acceptable.

Point-by-point responses to reviewers' comments

Changes are highlighted in blue in the revised manuscript.

Reviewer #1 (Remarks to the Author):
In the new version of the manuscript, authors have made an extraordinary effort and answered all the questions raised in the first version.

I have to acknowledge the great improvement of the work.
I am also glad that my suggestions have been positively used in the current manuscript.
In my view, this is an outstanding work and it will be of interest for a broad audience. Therefore, I strongly recommend this manuscript for publication in nature communications.

We thank the reviewer for the positive recognition of our efforts to revised the manuscript.

Reviewer #2 (Remarks to the Author):
The authors have addressed my substantive concerns, and I support publication in Nature Communications.

I have a few minor comments below.

Reviewer credentials for the PRIDE dataset were not provided.

We apologize the missing credentials. We originally set the entries to be publically accessible but the setting was not made as expected. Please find below the credentials for reviewers"

Username: reviewer_pxd064931@ebi.ac.uk
Password: NdpBk2gkaH7z

Username: reviewer_pxd064932@ebi.ac.uk
Password: BqzDK3CqGKo9

The revision appears to use an updated version of the analysis software (with fixes to FDR estimation and other bugs) that substantially improves the results relative to the original submission. However, several aspects of the experimental workflow remain unclear and may be suboptimal. Analyzing the 26S proteasome by SDS-PAGE or Western blot after crosslinking is feasible; if practical, please include a gel-based comparison of crosslinked and non-crosslinked samples (Western blot or stained gel). While optional, this addition would strengthen the manuscript.

The reviewer's recommendation to include the SDS-PAGE result of crosslinked samples is well taken. However, due to limited amount of material, we didn't analyze the sample with/without crosslinkers by SDS-PAGE or Western blot at the time. We fully agree that such data will be nice addition to the manuscript. We will make sure such information is recorded in the future.

Given reports that DSSO can yield elevated false-positive rates, it would strengthen the manuscript to include a figure mapping all identified crosslinks onto a high-resolution proteasome structure and to quantify overall reliability (e.g., the fraction of inter-subunit crosslinks across all proteasome subunits that satisfy expected distance constraints). This would be more informative than emphasizing the over-length crosslinks between RPN3 and the ubiquitin chain (Supplementary Fig. 10d).

We have incorporated the reviewer's suggestion to revise Supplementary Fig. 10 as follows:

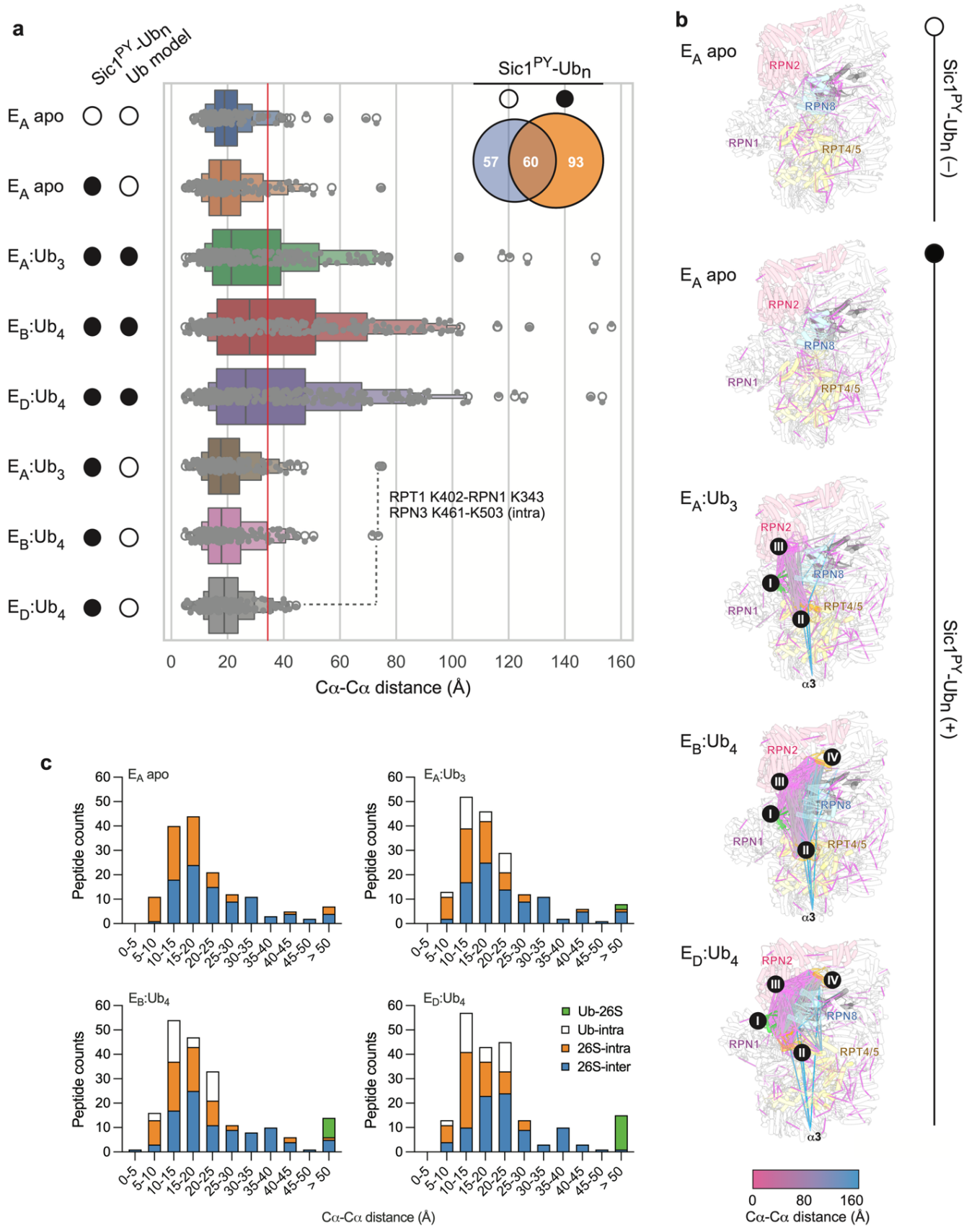
a
Sic1PY-Ubn
Ub model
EA apo
EA apo
EA:Ub3
EB:Ub4
ED:Ub4
EA:Ub3
EB:Ub4
ED:Ub4
Sic1PY-Ubn
57
60
93
RPT1 K402-RPN1 K343
RPN3 K461-K503 (intra)
0 20 40 60 80 100 120 140 160
Cα-Cα distance (Å)
b
EA apo
EA apo
EA:Ub3
EB:Ub4
ED:Ub4
RPN2
RPN8
RPN1
RPT4/5
α3
Sic1PY-Ubn (–)
Sic1PY-Ubn (+)
0 80 160
Cα-Cα distance (Å)
c
EA apo
EA:Ub3
EB:Ub4
ED:Ub4
Peptide counts
0-5 5-10 10-15 15-20 20-25 25-30 30-35 35-40 40-45 45-50 > 50
Ub-26S
Ub-intra
26S-intra
26S-inter
Cα-Cα distance (Å)

Supplementary Fig. 10. Structural mapping of XL-MS data onto the cryo-EM models of 26S proteasome. a, *Distance distributions of observed XL lysine pairs in different functional states – apo E_A (PDB entry: 8JRI), E_A:Ub_3 (PDB entry: 8JRT), E_B:Ub_4 (PDB entry: 8JTI) and E_D:Ub_4 (PDB entry: 8K0G) – without and with $Sic1^{PY}$-Ub_n indicated by open and filled circles, respectively, next to their functional states. The XL distances were mapped by XMAS as a plug-in module within ChimeraX. The distances are defined as the Cα-Cα distances between the lysines that are linked by DSSO. To highlight the long distances attributed to XL with Ubs, additional distance distributions were calculated for the E_A:Ub_3, E_B:Ub_4, and E_D:Ub_4 states, excluding the coordinates of the Ubs (bottom three rows), as indicated by open circles in the second column next to their functional state annotations. The generally accepted XL range of 35 Å is indicated by a red vertical line. Two long XL distances beyond 75 Å were observed in the E_A:Ub_3 and E_B:Ub_4 states, corresponding to an inter-chain XL of RPT1 K402-RPN1 K343 and an intra-chain XL of RPN3 K461-K503. These long XL distances were reduced to < 45 Å in the E_D:Ub_4 state, indicating that these XLs captured the conformation corresponding to the E_D:Ub_4 state distinct to the E_A:Ub_3 and E_B:Ub_4 states. Inset: Venn diagram of the overlap of the observed XL between the E_A states without (blue) and with (orange) $Sic1^{PY}$-Ub_n. Only 60 XLs were commonly observed in these two conditions, dominated by the shift of XLs corresponding to the supplemented UCHL5(C88A), RPN13, and Ub(K63R) in addition to $Sic1^{PY}$-Ub_n in the reconstituted 26S proteasome sample.* ***b,*** *Structural mapping of the observed XLs in the apo E_A (±$Sic1^{PY}$-Ub_n), E_A:Ub_3, E_B:Ub_4 and E_D:Ub_4 states rendered by XMAS using ChimeraX. The XL distances are color-ramped from fuchsia to blue, corresponding to 0 to 160 Å, as indicated by the scale bar on the bottom. The subunits of interests and Ub_I-Ub_{IV} are colored following the same scheme in Figure 1e (except RPN1 in white) and in highly transparent cartoon representations.* ***c,*** *Histogram of observed XL as a function of Cα-Cα distance in Å. The inter- and intra-subunit XLs within the 26S proteasome are colored blue and orange, respectively. The intra-subunit XLs within individual Ubs are colored white. The inter Ub-26S XLs are colored green. The majority of the long XLs (> 50Å) correspond to the inter Ub-26S XLs, which may be attributed to the assignments of the same 26S subunit linked to the multiple Ubs, evidenced by the only few XLs > 35 Å in E_A:Ub_3 where Ub_{IV} is absent in the structure. Source data are provided as a Source Data file.*

From the revised Supplementary Fig. 10c, it can be seen that all the intra-subunit XLs within the 26S are within 35 Å in the E_D:Ub_4 state while a relatively small number of inter-subunit XLs within the 26S are longer than 35 Å. Their distributions vary in different functional states, i.e., E_A apo, E_A:Ub_3, E_B:Ub_4 and E_D:Ub_4 states due to conformational changes, which are highlighted in Supplementary Fig. 10a as well. Furthermore, all intra-Ub XLs are within 35 Å. Only the inter Ub-26S XLs are often found to be longer than 50 Å, which could be attributed to (i) the issue of multiple Ubs of the same sequence in the protein models, (ii) the conformational variability within the 19S RP and the Ub chain, and (iii) the possible contributions from the additional Ub moieties extending from the core tetra Ub structure. Following the reviewer's recommendation, we hope the revised Supplementary Fig. 10c will provide assurance of the overall quality of the XL-MS data analyses without emphasizing the over-lengths of some XLs in the dataset.

Reviewer #3 (Remarks to the Author):

The authors have made a number of revisions to their manuscript and go some way to addressing my concerns about their interpretation of the densities they assign to the Ub4 molecule with their new supplementary figures. However, I remain concerned that the main text is still misleading with respect to the confidence with which they make their assignments. They continue to state that their interpretation derives from their ability to "unambiguously resolve the cryo-EM densities of a K11/K48-branched tetra-Ub (Ub4)". In my view the interpretation of their cryo-EM densities is far from unambiguous. They place considerable confidence in their assignment of individual densities to the extended C-terminal ubiquitin tails. Given that individual strands are not resolved in the beta-sheet regions of ubiquitin densities (supplementary fig R7), it is not clear that the details of the EM densities

they assign to the ubiquitin C-terminal tails can be relied on. This can be appreciated by considering the various panels of supplementary figure R7 in which the threshold chosen to maximise visibility of secondary structure elements within the globular domain ubiquitin domains leads to fragmented density for the C-terminal tails.

It would be better if the authors were to acknowledge that in this matter they are working close to the limits of resolution and signal to noise ratio. They would probably be justified in putting forward their model as being the most likely interpretation (comapred to alternatives) based on the various arguments presented in their new supplementary data, but I think they should explicitly make this argument in an objective fashion rather than claiming that each new observation confirms their original conclusion.

We appreciate the reviewer's reminder that we are working close to the limits of resolution. To address the reviewer's concern, we have modified our statement on page 4, second paragraph as follows to tone down our interpretation of the cryo-EM map.

"*Informed by the Ub-AQUA data that indicated the most abundant linkage types (Fig. 1d), we generated the atomic models of a K11/K48-branched tetra-Ub (Ub_4) chain bound to the E_B and E_D states (hereafter E_B:Ub_4 and E_D:Ub_4, respectively) (Fig. 1e-f), which showed good per-residue Q-scores[52] for the individual Ubs (Supplementary Fig. 6). The individual Ubs adopted unique spatial distributions with respect to the neighboring Ub to enable the modeling of the most probable isopeptide bond linkages when considering the conformational landscape accessible to Ub[53] (Supplementary Fig. 7).*"

We also removed the use of "unambigiously determined" and "unequivocally determined" in the Introduction and Discussion sections, respectively. We hope the reviewer will find the revised statement acceptable.